

The Isolation of Cellulose Nanocrystals from Pistachio Shells and Their Use in Water  
Actuating Smart Composites  
Josh Michael Marett

Thesis submitted to the faculty of the Virginia Polytechnic Institute and State University  
in partial fulfillment of the requirements for the degree of

Master of Science  
In  
Materials Science and Engineering

E Johan Foster. Chair  
Alexander O Aning  
Michael J Bortner

August, 11, 2017  
Blacksburg, Virginia

Keywords: Composites, Cellulose, Cellulose Nanocrystals

# The Isolation of Cellulose Nanocrystals from Pistachio Shells and Their Use in Water Actuating Smart Composites

Josh Michael Marett

## ABSTRACT

In recent years, there has been a significant amount of research into cellulose nanocrystals (CNCs). These materials are categorized as being between 5 and 10 nm wide and being 100-250 nm long. CNCs have several uses, but the most common is the reinforcement of polymer composites. Here I present 2 papers investigating CNC-based composites.

By using standard bleaching procedures, pure cellulose was isolated from pistachio shells. Sulfuric acid was used to isolate cellulose nanocrystals from the purified cellulose. The obtained crystals were investigated by scanning electron microscopy, transmission electron microscopy, and X-ray diffraction. The CNCs were also added to thermoplastic polyurethane (TPU) to observe the reinforcement effects by dynamic mechanical analysis. Pistachio shells offered a high yield source material for CNCs, with a high aspect ratio but a low crystallinity. They did offer significant reinforcement of the TPU, but less than the commercially available wood-based CNCs.

Wood-based CNCs were also mixed with TPU in structured composites to create a film which actuates when exposed to water. The method of actuation is based on the different amounts of absorption of water in the composite as opposed to the pure TPU. The actuation was modeled based on the absorption of water and the modulus of two components. Mechanical properties of the CNC/TPU composites were evaluated via dynamic mechanical analysis, and water absorption was measured gravimetrically. The tests helped us to evaluate our model which we compared to the composites.

# The Isolation of Cellulose Nanocrystals from Pistachio Shells and Their Use in Water Actuating Smart Composites

Josh Michael Marett

## GENERAL AUDIENCE ABSTRACT

Composites are a category of materials where two or more materials are used together to enhance each of their strengths. Such materials are often used in airplanes, spacecraft, sporting equipment, and many high-end products. Cellulose nanocrystals (CNCs) have been research with the goal of improving the environmental sustainability and performance of composite materials. This newly utilized material is found in plants and some animals to provide them with their strength. Researches have already shown that CNCs can improve the performance of many materials while reducing their lifetime environmental impact. In order to increase the market for CNCs, we are looking at cost-reducing methods of producing them as well as finding exciting new uses for them once they are made.

Right now, most CNCs are isolated from wood or cotton, which already have existing markets. This thesis presents a method of using pistachio shells, which are a waste product in many parts of the world including the United States. By finding new sources of CNCs, we hope to add to the body of knowledge and reduce the price of CNC production.

This thesis also lays the groundwork for a material that changes shape when exposed to water. By integrating CNCs into only part of a polymer, when water is added, the part with the CNCs will increase in size, causing it to push on the polymer. Our hope is to create a new use for CNC composites to help to increase the market for them. We

discuss potential methods and proofs of concept on how to create a 3D-printed part using CNCs and polyurethane.

## **Acknowledgements**

I would like to thank a great many people, without whom this thesis would not have been possible, but the page can only fit a few of them. I would like to thank my advisor, Dr. Johan Foster, for allowing me to work in the Advanced Materials Group. It has been an honor and a pleasure to be working on real problems with practical solutions in the group. I would also like to thank Dr. Foster for his guidance with my research, his ideas that have moved these projects forward, and his willingness to help at any opportunity. He has been an incredibly friendly and supportive advisor who has always given me the tools to succeed and time to relax.

I would also like to thank my other committee members, Dr. Alex Aning and Dr. Michael Bortner. They have each been uniquely helpful in this endeavor with their subject matter expertise on composite materials processing and evaluation as well as many other topics.

I would like to thank all of other members of the Advanced Materials Group at Virginia Tech. They have always been a wealth of knowledge and support for me, as well as offering me your friendship. I would like to thank, in no particular order: Rose, Kelly, Keith, Sean, Anara, Chris, Brody, Cameron, Fang, Priya, Steve, and Zahra. They have all been wonderful to work with, and I wish them all nothing but the best.

I would also like to thank the members of Polymer and Composite Research Laboratory for their help. I would especially like to thank Jake, who assisted me with attempting to 3D-print composite materials and helped me design molds for my projects. I know that I took up a fair amount of time in his already busy schedule and I thank him for working with me with a smile on his face and friendly and candid advice.

There are many members of the MSE department at Virginia Tech who have been helpful during this process. I would especially like to thank Dr. Thomas Staley for offering me my role as a TA. I have been blessed to work with many talented co-TAs who have been good friends. I would like to thank Ellen, Jerry, Manuel, James, and Amelia.

Finally, I would like to thank my fiancée, Micah, for always being understanding of my hours and providing me with countless hours of support and companionship. I would like to thank my family and friends for their support throughout the process.

## **Table of Contents**

<b>List of Figures</b>	<b>vii</b>
<b>List of Abbreviations</b>	<b>ix</b>
<b>Attribution</b>	<b>x</b>
<b>1 Introduction</b>	<b>1</b>
1.1 Composites	1
1.1.1 Fiber reinforced composites	2
1.1.2 Smart composites	5
1.1.3 CNC composites	8
1.2 Cellulose	9
1.2.1 History	10
1.2.2 Chemistry	10
1.2.3 Structure	11
1.2.4 Nanocellulose	13
1.3 References	20
<b>2 Problem Statement and Objective</b>	<b>26</b>
<b>3 The Isolation of Cellulose Nanocrystals from Pistachio Shells via Acid Hydrolysis</b>	<b>28</b>
3.1 Abstract	28
3.2 Introduction	29
3.3 Procedure and Materials	31
3.4 Results and Discussion	35
3.5 Conclusions	40
3.6 References	41
<b>4 Creating a Water Activated, Self-Folding Film from Cellulose Nanocrystals and Polyurethane</b>	<b>43</b>
4.1 Abstract	43
4.2 Introduction	43
4.3 Materials	45

4.4 Pressed films	45
4.4.1 Making pressed films	45
4.4.2 Testing pressed films	46
4.5 Printing films	47
4.5.1 Making printed films	47
4.5.2 Testing printed films	48
4.5.3 Changing the material	49
4.6 Compression molding	51
4.6.1 Making compression-molded films	51
4.6.2 Testing compression-molded films	52
4.7 Modeling	52
4.8 Future Recommendations	54
4.9 References	55
<b>5 Conclusions and Outlook</b>	<b>58</b>
5.1 Conclusions	58
5.2 Outlook	58



## **List of Figures**

<b>Figure 1.1</b>	A view of continuous fiber composite (left) and discontinuous fiber composites (right).	<b>3</b>
<b>Figure 1.2</b>	A schematic showing how 3D printing aligns fibers.	<b>5</b>
<b>Figure 1.3</b>	Types of smart composites. a) showing the use of matrix materials as damage sensors b) using zinc oxide whiskers on a carbon fiber for sensing application c) using different colors of ink and light to create shape memory	<b>7</b>
<b>Figure 1.4</b>	A view of how CNCs can be used to create a shape memory composite	<b>9</b>
<b>Figure 1.5</b>	The chemical structure of cellulose	<b>10</b>
<b>Figure 1.6</b>	A visual description of the structure of cellulose at different scales	<b>12</b>
<b>Figure 1.7</b>	Micrographs of CNCs by SEM (left) and TEM (right)	<b>14</b>
<b>Figure 1.8</b>	The different failure mechanisms of composites with CNCs and CNFs.	<b>19</b>
<b>Figure 3.1</b>	a: A pistachio in the shell. b: Milled shell. c: Post extraction cellulose. d: Dried	<b>36</b>
<b>Figure 3.2</b>	SEM image of isolated CNCs	<b>36</b>
<b>Figure 3.3</b>	TEM image of isolated CNCs	<b>37</b>
<b>Figure 3.4</b>	XRD spectra comparing crystallinity of pistachio shells, CNCs isolated from the pistachio shells, as well as commercially available CNCs for comparison	<b>38</b>
<b>Figure 3.5</b>	Dispersibility of CNCs after a) 0 hours, b) 0.5 hours, c) 12 hours, and d) 24 hours in water, DMF, DMSO, DCM, ethanol, and toluene.	<b>39</b>
<b>Figure 3.6</b>	Stress-strain plots showing pure TPU, TPU reinforced with either CNCs isolated from pistachio shells or commercially available CNCs isolated from wood	<b>40</b>
<b>Figure 4.1</b>	60 wt % CNC film before water was added (left), 15 minutes after water was added (center), and one hour after water was added.	<b>47</b>
<b>Figure 4.2</b>	A computer generated model showing the shape of the printed hinge with the blue being pure TPU and the green being the CNC/TPU composite	<b>48</b>

<b>Figure 4.3</b>	Showing composite filament before and after printing (left), and printed around TPU in a bi-layer film in its actuating state (right)	<b>49</b>
<b>Figure 4.4</b>	TGA of isolated CNCs	<b>50</b>
<b>Figure 4.5</b>	Rheometry of Texin and Soft 35 at various temperatures	<b>51</b>
<b>Figure 4.6</b>	Custom steel compression mold	<b>52</b>
<b>Figure 4.7</b>	a) Percent mass gained after various times in water, b) Mechanical testing of different wt% CNC composites, c) Model of maximum actuation of different thicknesses of different concentrations of CNC composites.	<b>54</b>

### **List of abbreviations**

<b>CNC</b>	<b>Cellulose nanocrystal</b>
<b>CNF</b>	<b>Cellulose nanofibril</b>
<b>TPU</b>	<b>Thermoplastic polyurethane</b>
<b>DMF</b>	<b>n,n-dimethylformamide</b>
<b>DMA</b>	<b>Dynamic mechanical analysis</b>
<b>XRD</b>	<b>X-ray diffraction</b>
<b>SEM</b>	<b>Scanning electron microscopy</b>
<b>TEM</b>	<b>Transmission electron microscopy</b>
<b>DI</b>	<b>De-ionized</b>
<b>DMSO</b>	<b>Dimethyl Sulfoxide</b>
<b>DCM</b>	<b>Dichloromethane</b>

## **Attribution**

Most of the work presented in this thesis is the work of me, Joshua Marett. The first paper is co-authored by Dr. Johan Foster and Dr. Alex Aning. They gave help understanding the results of my tests and assisted me when I was stuck by offering solutions which I then pursued. The second paper is co-authored by Mr. Jake Fallon, Dr. Johan Foster, and Dr. Michael Bortner. Jake was very helpful in preparing parts via 3D printing and working with me to design the compression mold. He also put in the order for the mold with the chemistry machine shop and ran the capillary rheometry tests. Dr. Foster and Dr. Bortner assisted me by determining the scope of the project and showing me several of the papers to point me in the right direction during the start of the project.

## **Chapter 1: Introduction**

There are many different factors to consider when designing a material. Often these include physical properties such as strength, stiffness, or density; thermal properties such as thermal expansion, thermal conductivity, and thermal degradation; and electrical properties such as magnetism, resistivity, or charge permeability. Each class of material tends to have specific properties, such as ceramics having high stiffness or metals offering high strength.<sup>1</sup> By combining two types of materials, it has been possible to get some of the advantages of each type of material; these are called composite materials.<sup>1</sup> Composite materials are typically categorized by high stiffness and low density, though they often are expensive and difficult to manufacture.<sup>2</sup>

### **1.1 Composites**

Composites are a class of material where two or more materials are put together to enhance their mechanical properties. Composites have primarily been used in the aerospace materials field due to their high strength, high fatigue resistance, and low density.<sup>3-4</sup> There are many different types of matrix-based composites noted by the type of reinforcement which includes fibers, whiskers, flakes, and particles.<sup>2</sup> Non-matrix types of composite are limited to sandwich and laminate composites.<sup>2</sup> Due to their complexity, composites have continued to be an area of significant materials research. In matrix-based composites, a wide variety of materials have been used as both the matrix and reinforcement material.<sup>2, 5-9</sup>

## **1.1.1 Fiber Reinforced Composites**

### **1.1.1.1 Continuous Fiber Composites**

The most well-understood type of composite material is aligned, continuous fiber reinforced polymer composite.<sup>1</sup> In this style of composite, the reinforcement material is a long fiber which increases the stiffness and strength of the material, especially in the direction of the fiber alignment. These composites are typically modeled by using a weighted average of the materials known as the rule of mixtures.<sup>1-2</sup> Aligned, continuous fibers have been researched in depth and have been known about for many years.<sup>10</sup> Advancements in this area are mostly in multi-functional composites or novel processing techniques. Multi-functional composites are discussed in section 1.1.2.

With the advent of additive manufacturing and the significant amount of research about it in the recent years, one goal has been a method of printing composite materials.<sup>7, 11-13</sup> Printing continuous fibers has led to much faster production times due to the ease of manufacturing.<sup>12, 14</sup> Some advantages of the additive techniques include helping to align the fibers, little to no post-processing, and a reduction in wasteful scrap material that traditional manufacturing creates.<sup>12, 14-15</sup> The goals of continued research in this area are to further reduce the time to create a part, incorporate new fibers or matrix materials, and increase the mechanical properties of the final part.<sup>12, 14-15</sup>

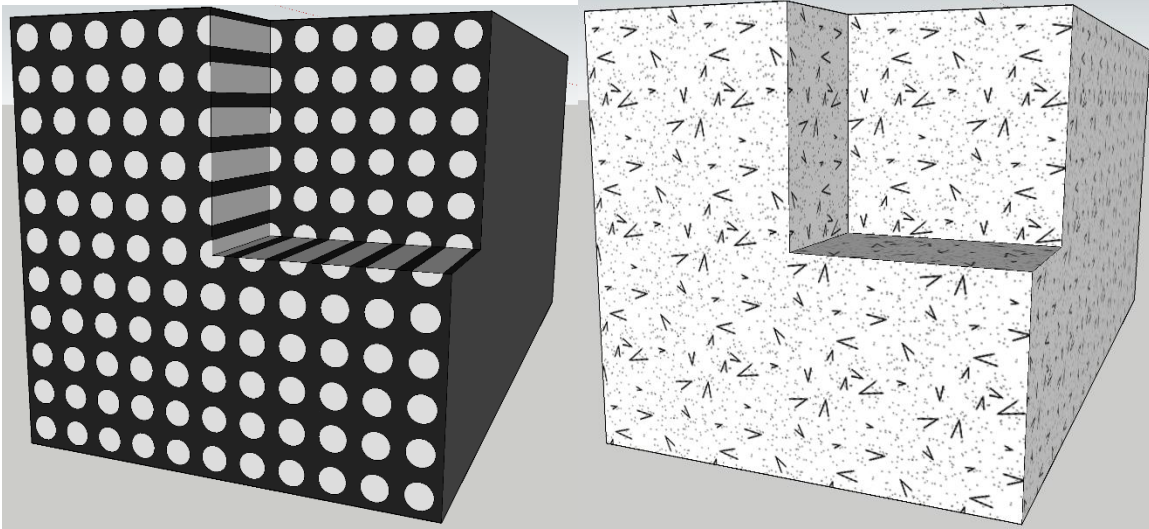


Figure 1.1. A view of continuous fiber composite (left) and discontinuous fiber composites (right).

### 1.1.1.2 Discontinuous Fiber Composites

Discontinuous (also known as short or chopped) fibers are significantly easier to make, but are more complicated to model than continuous fibers.<sup>16</sup> Although they do not add as much stiffness or strength as the continuous fiber composites, short fibers still increase resistance to creep, fatigue, and crack propagation.<sup>2</sup> They are significantly easier to produce because the fibers are not typically aligned and are much shorter.<sup>2</sup> Figure 1.1 above shows a cross-section of both continuous and discontinuous fiber reinforced matrix composites for comparison. A very common type of short fiber composite is epoxy matrix composite.<sup>4</sup> In this application, the toughness of the fiber drastically increases the fracture toughness of the part while making sure that the final part has the low density of the epoxy and is easy to produce.<sup>3-4</sup>

There has been a large volume of research in using short fiber composites for bio-medical applications.<sup>14, 17-18</sup> The goal of most bio-medical applications is to reproduce the numerous discontinuous fiber systems that are present in the human body.<sup>17-18</sup> These

topics range from skin grafts to bone replacements <sup>17-18</sup>. For this application, the main goal of adding fibers is to allow materials which were selected for their bio-inert properties, rather than their mechanical properties, to become strong enough to perform their role in the human body.<sup>17</sup> By adding the rigid fibers, the composites can be strong enough to replace bone. Wang et al accomplished a bone replacement by using carbon nanotubes in hydroxyapatite to create a solid bone implant.<sup>19</sup> Adding fibers as reinforcement in these cases can also increase the lifetime of composites by preventing crack propagation.<sup>19</sup> Another benefit of using composites in biomedical applications is the ability to carefully and easily control the mechanical properties by selecting the concentration of fiber in the composite to be able to use the same material system for bone and tissue implants.<sup>19</sup>

Like the longer continuous fibers, there is a significant amount of research dedicated to researching novel processing techniques for shorter fibers. Advances in additive manufacturing have led to a revival of interest in short-fiber composites.<sup>6, 20-21</sup> One major advantage that the 3D-printing technique of polymer extrusion has offered to discontinuous fiber composites is that it helps to align them, as shown in Figure 1.2 on the next page, which increases their stiffness and strength, but also creates anisotropy.<sup>6, 16</sup> This alignment has caused a surge of research into how to use this property to increase the mechanical properties of the printed part.<sup>22-23</sup>



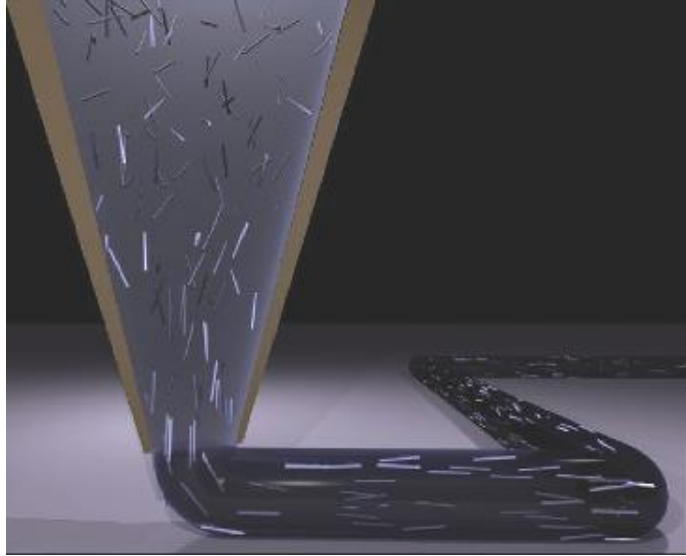


Figure 1.2: A schematic showing how 3D printing aligns fibers. Reprinted with permission from Compton et al <sup>24</sup>. Copyright 2014 WILEY-VCH Verlag GmbH & Co.

The research has focused on how to best use the aligned fibers to increase different types of strength, such as to eliminate the anisotropy of the system while reducing the maximum strength as little as possible.<sup>22</sup> Such designs are often called meso-scale materials design.<sup>25</sup> Meso-scale structures have already led to functionally gradient materials and new methods of optimizing the material properties.<sup>25</sup>

### **1.1.2 Smart composites**

A use of composite materials is stimuli-responsive composites, which are often referred to as smart materials. These materials have many different properties such as directional electrical conductivity, gas sensing, in-situ monitoring, and even creating movement in the part.<sup>26-31</sup>

#### **1.1.2.1 Self-sensing materials**

Smart materials are usually some form of composite where either a sensing element is added to the matrix material with fibers used to reinforce the part, or the fibers themselves act as both reinforcement and the sensor.<sup>26-31</sup> One example of the former case

is using the change in electrical resistance of the matrix material to observe the damage in the material.<sup>29</sup> As the material is damaged or stretched significantly, the electrical resistance of the matrix phase changes.<sup>29</sup> This methodology is the same concept as a strain gauge used in materials testing, but because there is no external device applied, it can be continuously monitored in situ.<sup>29</sup>

By far, the more common method of smart material is using the reinforcement, not the matrix, as a sensor. Work done by Celestani et al. using zinc oxide nanowire coated carbon fiber can detect not only strain in the system, but also gasses such as ethanol and carbon monoxide.<sup>27</sup> In this research, the oxide changes resistance when the gasses are present, and the carbon fiber acts as a wire to carry the current to a detector.<sup>27</sup> The same system can also heat itself to high temperatures by manipulating the electrical voltages on different fibers.<sup>27</sup> The benefit of a material like this is that it acts not only as a sensor for many different types of gas, but it also has all of the other advantages of a fiber composite such as high stiffness.

### **1.1.2.2 Actuating Composites**

A final type of emerging smart composite that I want to discuss is self-assembling composites. By using different material's properties of the different phases, researchers have found a few methods of creating composite structures that can change shape with some stimulus, also referred to as shape memory materials.<sup>30-31</sup> There are a few methods of creating shape memory materials, including shape memory alloys and chemically switchable polymers, but I will be focusing on shape memory composites. These materials are of interest because a lack of motors allows the parts to move in much smaller spaces and with more precise control.<sup>30-31</sup> In research from both Felton et al. and

Liu et al., heat causes a relaxation in a pre-stretched polymer film which causes the actuation, but they have found different methods of causing that heat.<sup>30-31</sup> Felton et al. focus on using electrical power and resistors to generate heat in their part, while Liu et al. use differently colored light to cause heat along certain colored areas of their film.<sup>30-31</sup>

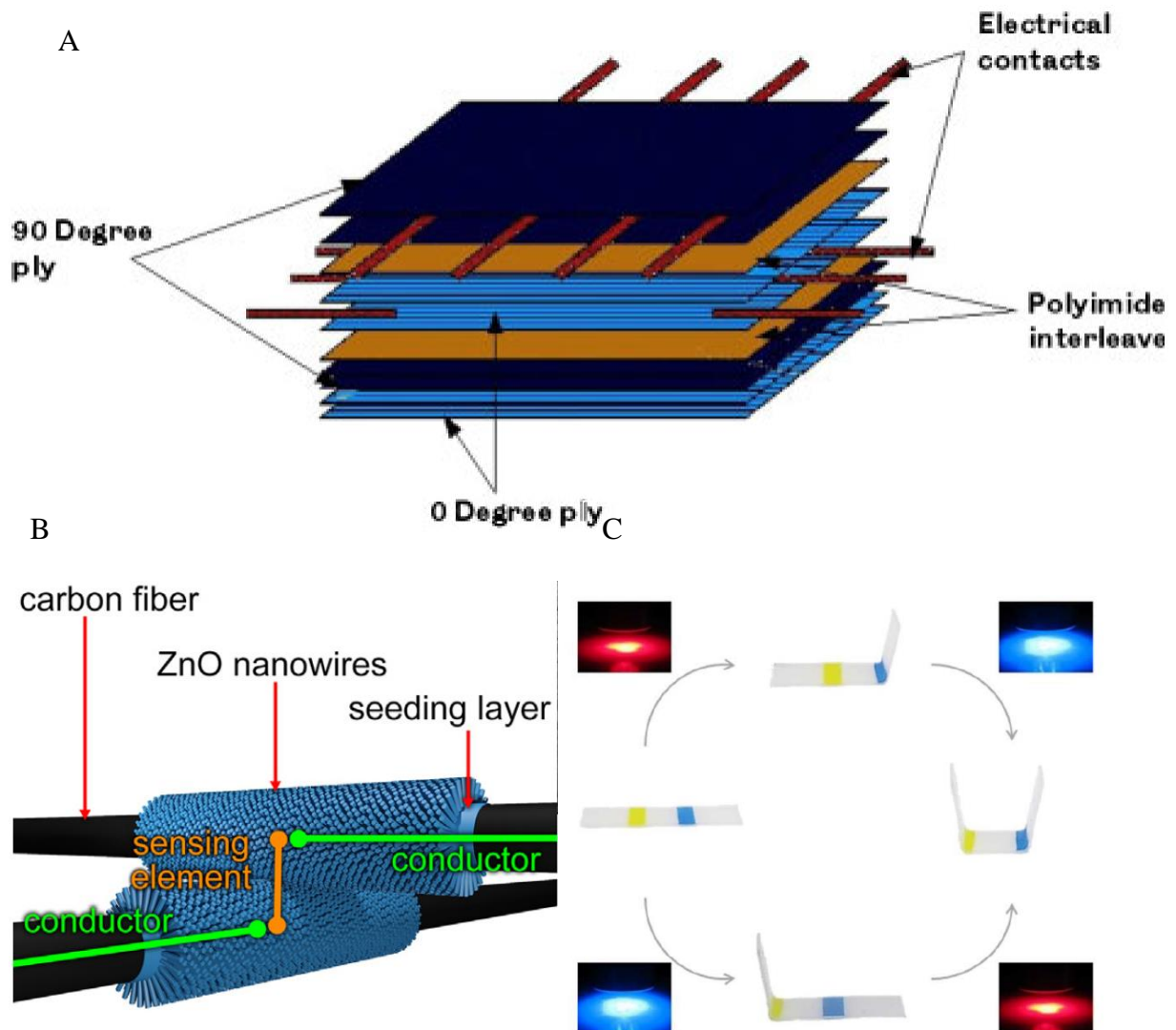


Figure 1.3: Types of smart composites. a) Use of matrix materials as damage sensors. Reprinted with permission from Swait et al.<sup>29</sup> Copyright 2013 Taylor & Francis. b) Zinc oxide whiskers on a carbon fiber for sensing application. Reprinted with permission from Calastani et al.<sup>27</sup> Copyright 2017 Elsevier. c) Using different colors of ink and light to create shape memory composites reprinted with permission from Liu et al.<sup>31</sup> Copyright 2017 Liu et al.

Other researchers have used differences in swelling behaviors to create the actuating motion.<sup>32-34</sup> These composite structures are made of two different materials with different swelling behaviors. The material that expands more with water presses against the material that expands less with water to create a bending action. Films that use this action range in size from micron scale several millimeters.<sup>33-34</sup> Depending on the scale and the materials used, swelling-based smart materials have a variety of functions from acting as a valve that changes based on different temperatures and liquids<sup>34</sup> to smart windows that automatically close in the rain<sup>35</sup>.

### **1.1.3 CNC Composites**

One type of reinforcement that has many different applications as a smart material and discontinuous reinforcement is the use of cellulose nanocrystals (CNCs). The primary use of CNCs is to reinforce many different polymers.<sup>36-43</sup> As stated above, stiff and strong discontinuous randomly aligned fibers are used to increase the stiffness, strength, and fatigue life of the composite.<sup>2,4</sup> The reason that CNCs are being researched is their high modulus to weight ratio.<sup>37,43</sup> With a modulus of between 100 and 200 GPa in the axial direction and a specific gravity of 1.6, CNCs compare with even ceramic particles such as aluminum oxide, which has a modulus of 380 GPa and a specific gravity of 4.<sup>43-44</sup> Comparing the two, we see that the specific modulus, the modulus divided by the specific gravity, for CNCs is between 62.5 and 125 GPa, while alumina has a specific modulus of 95 GPa.<sup>43-44</sup> CNCs are also a renewable resource that can be isolated from many plants.<sup>37,41,45-49</sup> Because it can be isolated from many different types of plants, it can be produced anywhere worldwide.

Cellulose nanocrystals have shown to have allow shape memory properties as well. Annamalai et al used the fact that CNCs are mechanically switchable to create a shape memory composite using a styrene-butadiene rubber.<sup>36</sup> Similar studies have been done using thermoplastic polyurethanes as well as other polymers.<sup>50</sup> Because of the hydrogen bonding nature of the crystals, the addition of water reduces the elastic modulus significantly, depending on the concentration of CNCs, to the point that the composite is easily manipulated.<sup>50</sup> By allowing the water to dry, the hydrogen bonding in the crystals is restored and the part will retain its new shape until it is re-wetted where it will return to its original shape as shown in figure 1.4.<sup>50</sup> The shape memory effect can be incredibly useful in many different applications.<sup>50</sup>

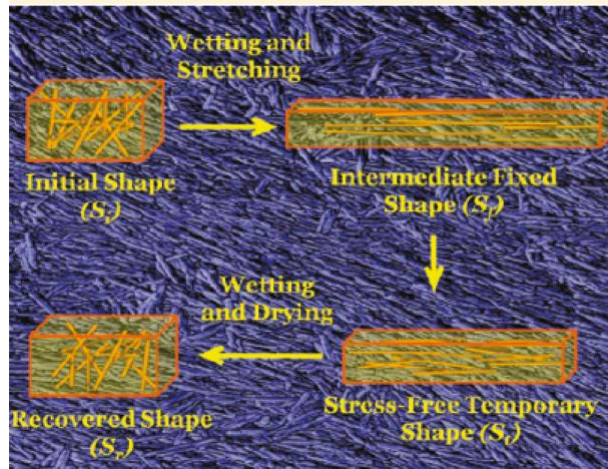


Figure 1.4: A view of how CNCs can be used to create a shape memory composite. Reprinted with permission from Mendez et al.<sup>50</sup> Copyright 2011 American Chemical Society.

## 1.2 Cellulose

Cellulose is the world's most abundant polymer with an estimated  $10^{10}$  and  $10^{12}$  tons produced annually.<sup>51-52</sup> It is most commonly found in the cell walls of plants, though cellulose has been found in some bacteria and some animals.<sup>37, 43, 53-55</sup>

### 1.2.1 History

Anselme Payne is credited with discovering cellulose in 1838.<sup>52, 56</sup> Payne was replicating a similar experiment done four years earlier by Braconnot, another French chemist, where he used nitric acid to create what we now know as nitrocellulose.<sup>52</sup> Payne found the same fibrous material after exposing many different plants to an acid-ammonia and then purifying the result with water, alcohol, and ethers.<sup>52</sup> Over the next 100 years, many different theories emerged about the structure of cellulose based on the molecular weight and as new theories on polymers were developed until finally in 1922 Staudinger and Fritsch figured out that the structure that we use today.<sup>52, 57</sup>

### 1.2.2 Chemistry

The formula of the monomer that makes up cellulose, cellobiose, is  $C_{12}O_{10}H_{20}$  in the structure of two glucose molecules connected by an oxygen through a (1-4)  $\beta$  bond.<sup>52, 55</sup> as shown in figure 1.5.<sup>43</sup> The structure is easily comparable to other biopolymers such as starch, which differs with the connection of the glucose blocks using both (1-4)  $\alpha$  bonds and (1-6)  $\alpha$  bonds.<sup>58</sup>

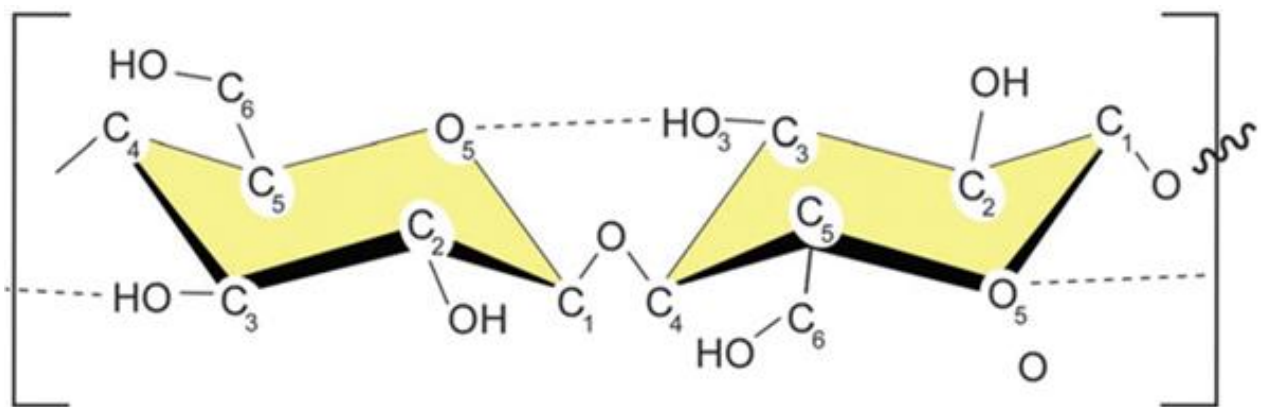


Figure 1.5: The chemical structure of cellulose. Reprinted with permission from Moon et al.<sup>43</sup> Copyright 2011 Royal Society of Chemistry.

There have been many chemical modifications to cellulose. The primary method for modification is by manipulating the hydroxyl group attached to carbon 6 via an acid,

alcohol, or other reactive group as well as something with which to replace the hydroxyl.<sup>43</sup> Such treatments have led to many different types of cellulose modification including grafting polymers<sup>59</sup>, altering rheological behavior<sup>60</sup>, and modifying dispersibility<sup>43</sup>.

### **1.2.3 Structure**

Cellulose naturally grows in the cell walls of plants as a fiber in a composite material known as lignocellulose.<sup>43</sup> Lignocellulose has continuous cellulose fibers in a matrix of lignin with hemicellulose acting to strengthen the bond between the two.<sup>43</sup> The cellulose fibers are further broken down into smaller fibrils, which are only a few nanometers in diameter and are in turn divided into amorphous and crystalline regions.<sup>43</sup> A schematic of the system is shown in figure 1.6 on the next page.<sup>61</sup>

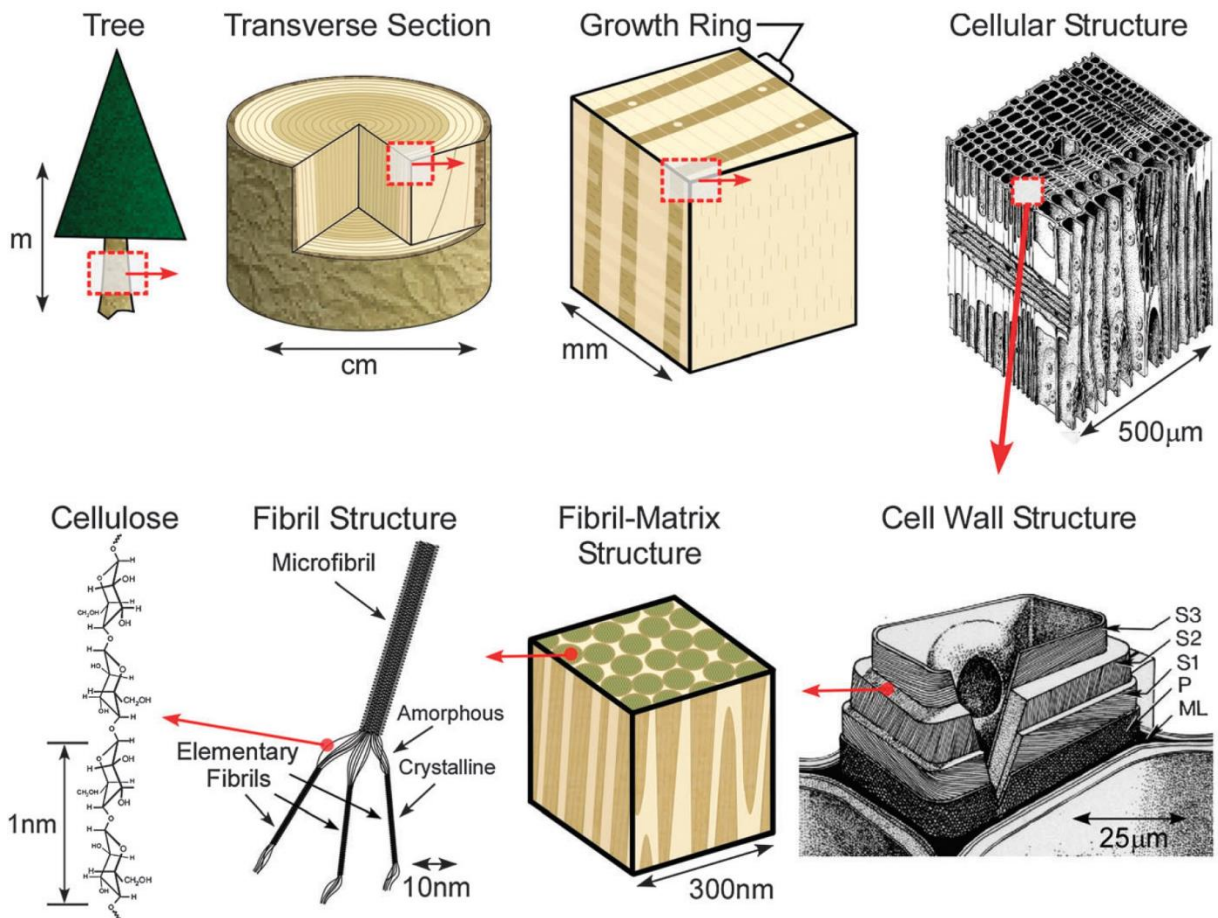


Figure 1.6: A visual description of the structure of cellulose at different scales. Reprinted with permission from Michael et al.<sup>61</sup> Copyright 2011 IOP Publishing Ltd.

The idea of crystalline cellulose is a relatively recent development. Around the same time that the chemistry and conformation of cellulose were being finalized, studies were just starting to look at its crystallinity via X-ray experiments.<sup>52</sup> There continue to this day to be advancements in our understanding of the crystalline structure of cellulose.<sup>62</sup> The natural form of cellulose, cellulose I, has linear fibers that are bound together via hydrogen bonding.<sup>55</sup> Cellulose I is metastable, which is to say that it will not spontaneously change to another form, but it is not at its lowest energy state.<sup>55</sup> Once the cellulose is dispersed in water or chemically treated, it can irreversibly change into cellulose II.<sup>43, 55</sup> Unlike cellulose I, cellulose II has a folded chain structure that bonds to



itself, resulting in a larger crystal.<sup>55</sup> Cellulose III and IV are both created by reversible reactions with cellulose III being hexagonal and cellulose IV being orthogonal.<sup>55</sup> Most of the research is done on either cellulose I or II as they are the most common.<sup>55</sup> For all structures, the crystalline domains of cellulose are nano-sized and surrounded by small amounts of amorphous cellulose.

## **1.2.4 Nanocellulose**

### **1.2.4.1 History**

By using polarized light microscopy, Nageli was the first to determine that cellulose was partially crystalline in 1858, only 20 years after cellulose was first discovered.<sup>55, 63</sup> It was not until powder x-ray diffraction was used on cellulose in the 1910's to 1930's that the crystals were confirmed and characterized.<sup>52, 55</sup> Even the earliest theories on cellulose microstructure had crystalline and amorphous regions with the idea of rod-like crystals being connected by un-ordered cellulose appearing in 1914 in a paper by Nishikawa.<sup>52, 64</sup>

Work done in the 1940s by Nickerson and Habrle, as well as many others, developed a method of hydrolyzing cellulose in an acid solution using hydrochloric acid and ferric chloride, resulting in a short period of rapid hydrolysis which rapidly slows down.<sup>65-66</sup> This method is nearly the same process as we use today to create cellulose nanocrystals (CNCs). Using palladium-shadowing to show higher contrast, Morehead was the first to image CNCs using an SEM to confirm the theory of rod-like particles.<sup>67</sup> It was not until 1995 that Favier et al used CNCs to reinforce polymers into composites.<sup>37, 68</sup> In that paper, CNCs from tunicates were used to reinforce latex to

increase the storage modulus.<sup>68</sup> Since then, CNCs have been used to reinforce several different polymers including polyethylene, polyurethane, polyester.<sup>39-40, 42</sup>

#### 1.2.4.2 Structure

It has been observed that using acid will dissolve the amorphous regions of cellulose, leaving just the highly crystalline whiskers.<sup>45-46, 48-49, 69</sup> While the chemical structure of CNCs is the same as that bulk cellulose, the mechanical properties are very different. While still in the lignocellulose structure, CNCs have a rectangular cross section surrounded by amorphous cellulose.<sup>43</sup> The CNCs are isolated by use of acid hydrolysis, which dissolves the crystalline portions slower than the non-crystalline portions, but it also changed the morphology of the CNC from a rectangle to that of a cylinder as shown in figure 1.7.<sup>43</sup>

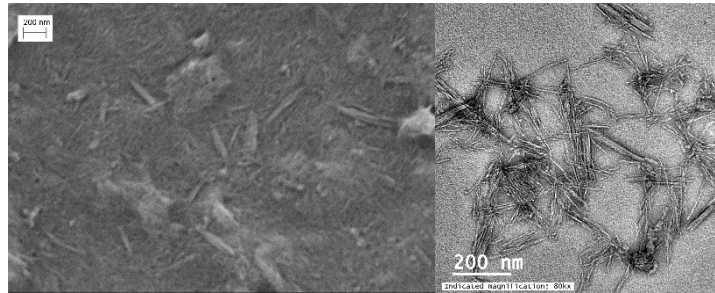


Figure 1.7: Micrographs of CNCs by SEM (left) and TEM (right)

The unique structure of CNCs offers many benefits. The first is the alignment of the hydroxyl groups which act as hydrogen bonding sites. This phenomenon allows the crystals to be suspended in polar solvents which can attach via the hydrogen bonding sites. It also allows for some solvents, such as water, to be readily pulled into CNC-based foams and composites.<sup>70</sup> Thus, although the bulk of the CNCs do not swell, the surface of the crystal can still hold a lot of water. Also, because the OH groups are

aligned, it is possible to align the crystals through a strong magnet while they are in suspension.<sup>71</sup> Aligning the crystals helps to further increase stiffness in one direction and to create anisotropic swelling properties. Additionally, the high aspect ratio of CNCs is very useful in making composites. Having a higher aspect ratio, increases the effectiveness of fiber reinforcements in composites.<sup>41</sup>

#### **1.2.4.3 Mechanical Properties**

CNCs are effective as a reinforcement agent in composites because they have a very high modulus themselves, up to around 100-200 GPa.<sup>43</sup> The high modulus is because the alignment of the hydroxyl groups in the crystal creates a lot of hydrogen bonding sites, which are known to increase stiffness in polymer crystals. These bonds also allow for the mechanical switching discussed previously, where the cellulose bonds to water molecules rather than to itself.<sup>72</sup>

Many of the physical characteristics of CNCs are dependent on the source of the cellulose.<sup>37</sup> The tunicate, a sea invertebrate, is commonly thought to be among the best sources of CNCs to use in composites, but it can be very costly to harvest due to the environment in which they grow.<sup>37, 73</sup> The most common sources of cellulose come from either wood or cotton due to the market abundance of the source material, high concentration of cellulose in the material, and the high aspect ratio and crystallinity of the CNCs. There have been other sources investigated including banana pseudostems,<sup>49</sup> pineapple leaf,<sup>74</sup> rice straw,<sup>48</sup> corncob,<sup>41</sup> soy hull,<sup>69</sup> and menkuang leaves,<sup>47</sup> each with their own physical properties. New sources are investigated regularly in an attempt to increase market diversity and lower cost. It is generally believed that high aspect ratio

and high crystallinity are particularly important in aiding the mechanical properties of CNC-reinforced composites, with crystallinity being the most important factor.<sup>41</sup>

#### 1.2.4.4 Uses

Because of the unique structure of CNCs, there are many ways CNCs can be used. The three primary uses for CNCs are to use them as a reinforcement for polymer matrix composites, to behave as a rheological modifier, and to stabilize emulsions.<sup>43, 68, 75-76</sup> The most common use is using them to increase the Young's modulus of various composites.<sup>41, 48-49, 69</sup> Even at low concentrations of CNCs, the storage modulus can be increased by an order of magnitude for some polymers.<sup>37</sup> A very large number of studies have been conducted on adding CNCs to a large number of polymers, both thermoplastics and thermosets for mechanical reinforcement.<sup>37</sup> There are many factors for how well CNCs affect the mechanical properties of composites including the crystallinity, aspect ratio, morphology, orientation, processing method, and interactions with the matrix.<sup>37</sup>

As mentioned above, there has also been significant research on creating mechanically switchable “smart” composites. Such films, often inspired by plants and animals, like the sea cucumber, CNC composites can have high stiffness when dry and can lower their storage modulus by over a factor of 10 with the addition of water.<sup>50, 72</sup> A critical advantage that CNC composites have with this mechanism of mechanical switchability is that it is reversible, and once the water is removed, the composite returns to its original stiffness, even after multiple cycles.<sup>50, 72</sup>

CNCs have also been used as a rheological modifier to create shear thinning gels.<sup>37, 77</sup> The shear thinning effect is attributed to the alignment of the crystalline domains with the direction of the flow, as is typical for shear thinning behaviors.<sup>37, 77</sup> It

has been noted that at higher shear rates, a shear thickening effect happens when the domains begin to break, and individual crystals affect the viscosity.<sup>37</sup> At very high shear rates when the individual crystals can be aligned and it returns to a shear thinning behavior<sup>37</sup>.

A more recent application of CNCs is to use them as a surfactant in emulsions.<sup>76</sup>  
<sup>78</sup> Researches have studied several different Pickering emulsions of oil and water from natural and synthetic oils.<sup>76,78-82</sup> The aligned hydrogen bonds creates a hydrophilic edge along the dimensions with hydroxyl groups while the other edges are hydrophobic<sup>76</sup>. This unique structure allows CNCs to stabilize the oil/water interface with or without added surfactants for months.<sup>76,79</sup> The added stability that the CNCs offer prevent the oil droplets from combining despite it being favorable for them to do so.<sup>76</sup> Keeping the oil drops small is important for many products including pharmaceuticals, cleaning agents and foods, all of which can be enhanced by the improved suspensions offered by CNCs.<sup>76</sup>

There are other, less researched uses of CNCs. UPM, a Finnish paper manufacturer has put forth a patent to use CNCs to increase the strength of its paper products.<sup>51</sup> It plans on using the strength to reduce the required thickness of the paper, lowering the weight.<sup>83</sup> Other researchers have looked at using CNCs in air and water filters to apparent success.<sup>51</sup> The size and high aspect ratio of the CNCs create very small pores which can capture even very small contaminates.<sup>51</sup> The optically transparent nature of CNC films has prompted some companies to look at using CNCs to create transparent displays.<sup>51</sup> Often these applications use CNCs for their environmentally friendly production method, as they are a plant-based product, in addition to one or more other properties.

#### 1.2.4.5 Types of Nanocellulose

There are two major types of nanoscale cellulose, cellulose nanofibrils (CNFs) and cellulose nanocrystals (CNCs).<sup>43, 67, 84</sup> Although they are both forms of nanocellulose, they are quite different. CNFs are physically separated fibrils which contain both the crystalline and amorphous regions of the cellulose fiber.<sup>43, 84</sup> CNCs are chemically separated through acid hydrolysis and are only the crystal domains of the cellulose fibers.<sup>43, 84</sup> Because of their different structures, they have very different uses. CNCs have a much higher crystallinity as almost all of the amorphous regions are gone, which leads to a higher Young's modulus.<sup>84</sup> Conversely, CNFs also have a much lower aspect ratio of about 8 while CNFs have an aspect ratio closer to 50.<sup>84</sup>

Their different morphologies offer different advantages when used in composites. Because of the CNFs high length, the yield strength increases more than CNCs as more of the fibers can be fully loaded.<sup>84</sup> However, at higher concentrations, CNFs entangle in each other, which can help make up for their low modulus, but can cause them to break each other<sup>84</sup>. As the composite starts to fail, CNFs allow for more fiber bridging, which can help stop crack propagation.<sup>84</sup> Both types of nanocellulose do show some fiber bridging, work hardening, and fiber pull-out, all of which increase the toughness of the composite as shown in figure 1.8 on the next pages.<sup>84</sup>

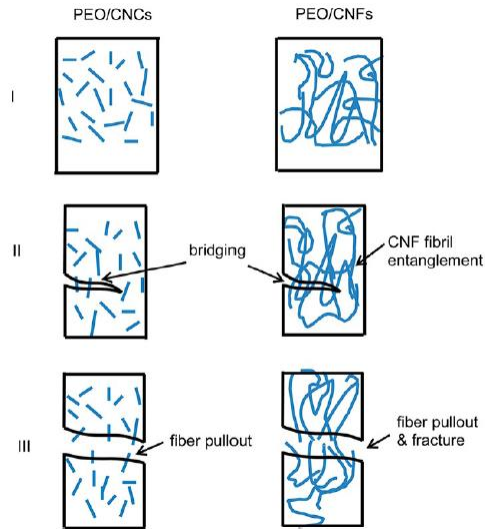


Figure 1.8: The different failure mechanisms of composites with CNCs and CNFs. Reprinted with permission from Xu et al<sup>84</sup>. Copyright 2013 American Chemical Society.

Like CNCs, CNFs have been used as a rheology modifier.<sup>85-86</sup> CNFs can increase the viscosity of water by several orders of magnitude to create stable gels with less than 1 wt% added.<sup>85</sup> Like CNCs, the gels created by CNFs are shear thinning, but because they lack the liquid crystal property of the CNCs, there is no shear thickening region but the increase in viscosity is not as high.<sup>85</sup> CNFs have also been looked into to stabilize emulsions.<sup>76, 87</sup> Because of the large size of the fibers, the droplet size in the emulsion is also much larger than when they are stabilized using CNCs.<sup>76</sup>

### 1.2.5.6 Nanocellulose Market

There is an emerging market for nanocellulose materials, but most of it is still far from mass manufacturing.<sup>88</sup> There are still a few problems with using CNCs and CNFs in commercial products, including developing more products which use the unique properties of nanocellulose and finding ways to use the fibers to their fullest effect. This can include more research into properly using the chemistry of cellulose.<sup>89</sup> Despite these hurdles, the biggest obstacle to large-scale production of cellulose nanomaterials is their

cost of production.<sup>88,90</sup> At the present, there are only a few refineries that make nanocellulose, and only the largest one is able to produce ton per day capacity.<sup>88</sup> The scarcity of CNCs on the market has raised the price to around \$1000/kg. The speed of commercialization will increase as the price falls. Experts report a goal of between \$4 and \$11 per kg before full market penetration occurs.<sup>90</sup> To this end, some researchers have been determining an alternate feedstock material for the bio-refineries to use.<sup>41, 47-49, 69,74</sup> The hope is to find sources of CNCs that are currently a waste product so that the refineries do not have to buy the costlier wood and cotton that they currently use.

### 1.3 References

1. Callister, W. D., Jr.; Rethwisch, D. G., *Materials science and engineering : an introduction*. 9th edition. ed.; Wiley: Hoboken, NJ ;, 2014.
2. Chawla, K. K., *Composite materials: science and engineering*. Springer Science+Business Media: New York, 2012; Vol. 3rd;3rd 2012;.
3. Li, Y. L.; Wang, W. X.; Zhou, J.; Chen, H. S.; Zhao, J. C.; Wang, B. D., Fatigue Crack Growth and Fracture of 30 wt% B4C/6061Al Composites. *Fatigue & Fracture of Engineering Materials & Structures* **2017**, n/a-n/a.
4. Srivastava, I.; Koratkar, N., Fatigue and fracture toughness of epoxy nanocomposites. *JOM* **2010**, *62* (2), 50-57.
5. Saheb, D. N.; Jog, J. P., Natural fiber polymer composites: A review. *Advances in Polymer Technology* **1999**, *18* (4), 351-363.
6. Harris, P. J. F.; Harris, P. J. F., Carbon nanotube composites. *International materials reviews* *49* (1), 31-43.
7. Azarov, A. V.; Azarov, A. V.; Antonov, F. K.; Vasil; rsquo; ev, V. V.; Golubev, M. V., Development of a two-matrix composite material fabricated by 3D printing. *Polymer science. Series D, Glues and sealing materials* *10* (1), 87-90.
8. Bhaduri, S.; Bhaduri, S. B., Recent developments in ceramic nanocomposites. *JOM* **1998**, *50* (1), 44-51.
9. Badev, A.; Abouliatim, Y.; Chartier, T.; Lecamp, L.; Lebaudy, P.; Chaput, C.; Delage, C., Photopolymerization kinetics of a polyether acrylate in the presence of ceramic fillers used in stereolithography. *Journal of Photochemistry and Photobiology A: Chemistry* **2011**, *222* (1), 117-122.
10. Sendeckyj, G. P.; Wang, S. S.; Steven Johnson, W.; Stinchcomb, W. W., Mechanics of Composite Materials: Past, Present, and Future. *Journal of composites technology & research* **1989**, *11* (1), 3.
11. Dong, L.; Shengyu, J.; Feng, Z.; Chao, W.; Yiqian, W.; Chi, Z.; Gary, J. C., 3D stereolithography printing of graphene oxide reinforced complex architectures. *Nanotechnology* **2015**, *26* (43), 434003.



12. Matsuzaki, R.; Ueda, M.; Namiki, M.; Jeong, T.-K.; Asahara, H.; Horiguchi, K.; Nakamura, T.; Todoroki, A.; Hirano, Y., Three-dimensional printing of continuous-fiber composites by in-nozzle impregnation. *Scientific Reports* **2016**, *6*, 23058.
13. Robert McCutcheon, R. P., Bobby Bobo, Mark Thut, 3D Printing and the New Shape of Industrial Manufacturing. PricewaterhouseCoopers, T. M. I., Ed. 2014.
14. Singh, S.; Ramakrishna, S.; Singh, R., Material issues in additive manufacturing: A review. *Journal of Manufacturing Processes* **2017**, *25*, 185-200.
15. Wong, K. V.; Hernandez, A., A Review of Additive Manufacturing. *ISRN Mechanical Engineering* **2012**, *2012*, 1-10.
16. Tucker Iii, C. L.; Liang, E., Stiffness predictions for unidirectional short-fiber composites: Review and evaluation. *Composites Science and Technology* **1999**, *59* (5), 655-671.
17. Wang, M., Developing bioactive composite materials for tissue replacement. *Biomaterials* **2003**, *24* (13), 2133-2151.
18. Thomson, R. C.; Yaszemski, M. J.; Powers, J. M.; Mikos, A. G., Hydroxyapatite fiber reinforced poly( $\alpha$ -hydroxy ester) foams for bone regeneration. *Biomaterials* **1998**, *19* (21), 1935-1943.
19. Wang, W.; Zhu, Y.; Liao, S.; Li, J., Carbon Nanotubes Reinforced Composites for Biomedical Applications. *BioMed Research International* **2014**, *2014*, 14.
20. Jue, J.; Gu, D., Selective laser melting additive manufacturing of in situ Al<sub>2</sub>Si<sub>4</sub>O<sub>10</sub>/Al composites: Microstructural characteristics and mechanical properties. *Journal of Composite Materials* **2017**, *51* (4), 519-532.
21. Sandoval, J. H.; Soto, K. F.; Murr, L. E.; Wicker, R. B., Nanotailoring photocrosslinkable epoxy resins with multi-walled carbon nanotubes for stereolithography layered manufacturing. *Journal of Materials Science* **2007**, *42* (1), 156-165.
22. Studart, A. R., Additive manufacturing of biologically-inspired materials. *Chemical Society Reviews* **2016**, *45* (2), 359-376.
23. Mahajan, C.; Cormier, D., 3D Printing of Carbon Fiber Composites With Preferentially Aligned Fibers. *IIE Annual Conference. Proceedings U6 - ctx\_ver=Z39.88-2004&ctx\_enc=info%3Aofi%2Fenc%3AUTF-8&rft\_id=info%3Aaid%2Fsummon.serialssolutions.com&rft\_val\_fmt=info%3Aofi%2Ffmt%3Akev%3Amtx%3Ajournal&rft.genre=article&rft.atitle=3D+Printing+of+Carbon+Fiber+Composites+With+Preferentially+Aligned+Fibers&rft.jtitle=IIE+Annual+Conference.+Proceedings&rft.au=Chaitanya+Mahajan&rft.au=Denis+Cormier&rft.date=2015-01-01&rft.pub=Institute+of+Industrial+and+Systems+Engineers+%28IISE%29&rft.spage=2953&rft.externalDocID=4070058371&paramdict=en-US* **2015**, 2953.
24. Compton, B. G.; Lewis, J. A., 3D-Printing of Lightweight Cellular Composites. *Advanced Materials* **2014**, *26* (34), 5930-5935.
25. Yu, H. Z.; Hang, Z. Y.; Samuel, R. C.; Christopher, A. S., Mesostructure optimization in multi-material additive manufacturing: a theoretical perspective. *Journal of materials science* **52** (8), 4288-4298.

26. Abdollahi, A.; Rad, J. K.; Mahdavian, A. R., Stimuli-responsive cellulose modified by epoxy-functionalized polymer nanoparticles with photochromic and solvatochromic properties. *Carbohydrate Polymers* **2016**, *150*, 131-138.
27. Calestani, D.; Villani, M.; Culiolo, M.; Delmonte, D., Smart composites materials: A new idea to add gas-sensing properties to commercial carbon-fibers by functionalization with ZnO nanowires. *Sensors and actuators. B, Chemical* **245**, 166-170.
28. Leng, J.; Asundi, A., Structural health monitoring of smart composite materials by using EFPI and FBG sensors. *Sensors and actuators. A. Physical.* **2003**, *103* (3), 330-340.
29. Swait, T. J.; Rauf, A.; Grainger, R.; Bailey, P. S.; Lafferty, A. D.; Fleet, E. J.; Hand, R. J.; Hayes, S. A., Smart composite materials for self-sensing and self-healing. *Plastics, Rubber & Composites* **2012**, *41* (4/5), 215-224.
30. Felton, S. M.; Tolley, M. T.; Shin, B.; Onal, C. D.; Demaine, E. D.; Rus, D.; Wood, R. J., Self-folding with shape memory composites. *Soft Matter* **2013**, *9* (32), 7688-7694.
31. Liu, Y.; Shaw, B.; Dickey, M. D.; Genzer, J., Sequential self-folding of polymer sheets. *Science Advances* **2017**, *3* (3).
32. Kokkinis, D.; Schaffner, M.; Studart, A. R., Multimaterial magnetically assisted 3D printing of composite materials. *Nature Communications* **2015**, *6*, 8643.
33. Guan, J.; He, H.; Hansford, D. J.; Lee, L. J., Self-Folding of Three-Dimensional Hydrogel Microstructures. *The Journal of Physical Chemistry B* **2005**, *109* (49), 23134-23137.
34. Gargava, A.; Arya, C.; Raghavan, S. R., Smart Hydrogel-Based Valves Inspired by the Stomata in Plants. *ACS Applied Materials & Interfaces* **2016**, *8* (28), 18430-18438.
35. He, S.; Chen, P.; Qiu, L.; Wang, B.; Sun, X.; Xu, Y.; Peng, H., A Mechanically Actuating Carbon-Nanotube Fiber in Response to Water and Moisture. *Angewandte Chemie (International ed. in English)* **2015**, *54* (49), 14880-14884.
36. Annamalai, P. K.; Dagnon, K. L.; Monemian, S.; Foster, E. J.; Rowan, S. J.; Weder, C., Water-Responsive Mechanically Adaptive Nanocomposites Based on Styrene-Butadiene Rubber and Cellulose Nanocrystals—Processing Matters. *ACS Applied Materials & Interfaces* **2014**, *6* (2), 967-976.
37. Dufresne, A., *Nanocellulose: from nature to high performance tailored materials*. De Gruyter: Berlin;Boston, 2012; Vol. 1. Aufl.
38. Habibi, Y.; Lucia, L. A.; Rojas, O. J., Cellulose Nanocrystals: Chemistry, Self-Assembly, and Applications. *Chemical Reviews* **2010**, *110* (6), 3479-3500.
39. Kargarzadeh, H.; M. Sheltami, R.; Ahmad, I.; Abdullah, I.; Dufresne, A., Cellulose nanocrystal: A promising toughening agent for unsaturated polyester nanocomposite. *Polymer* **2015**, *56*, 346-357.
40. Pei, A.; Malho, J.-M.; Ruokolainen, J.; Zhou, Q.; Berglund, L. A., Strong Nanocomposite Reinforcement Effects in Polyurethane Elastomer with Low Volume Fraction of Cellulose Nanocrystals. *Macromolecules* **2011**, *44* (11), 4422-4427.
41. Silvério, H. A.; Neto, W. P. F.; Dantas, N. O.; Pasquini, D., Extraction and characterization of cellulose nanocrystals from corncob for application as reinforcing agent in nanocomposites. *Industrial Crops and Products* **2013**, *44*, 427-436.

42. Sapkota, J.; Jorfi, M.; Weder, C.; Foster, E. J., Reinforcing Poly(ethylene) with Cellulose Nanocrystals. *Macromolecular Rapid Communications* **2014**, *35* (20), 1747-1753.
43. Moon, R. J.; Martini, A.; Nairn, J.; Simonsen, J.; Youngblood, J., Cellulose nanomaterials review: structure, properties and nanocomposites. *Chemical Society reviews* **2011**, *4* (7), 3941-3994.
44. Callister, W. D., Jr., *Fundamentals of materials science and engineering: an integrated approach*. John Wiley & Sons: Hoboken, NJ, 2005; Vol. 2nd.
45. Bondeson, D.; Mathew, A.; Oksman, K., Optimization of the isolation of nanocrystals from microcrystalline cellulose by acid hydrolysis. *Cellulose* **2006**, *13* (2), 171-180.
46. Kumar, A.; Negi, Y. S.; Choudhary, V.; Bhardwaj, N. K., Characterization of Cellulose Nanocrystals Produced by Acid-Hydrolysis from Sugarcane Bagasse as Agro-Waste. *Journal of Materials Physics and Chemistry* **2014**, *2* (1), 1-8.
47. Sheltami, R. M.; Abdullah, I.; Ahmad, I.; Dufresne, A.; Kargarzadeh, H., Extraction of cellulose nanocrystals from mengkuang leaves (*Pandanus tectorius*). *Carbohydrate Polymers* **2012**, *88* (2), 772-779.
48. Lu, P.; Hsieh, Y.-L., Preparation and characterization of cellulose nanocrystals from rice straw. *Carbohydrate Polymers* **2012**, *87* (1), 564-573.
49. Mueller, S.; Weder, C.; Foster, E. J., Isolation of cellulose nanocrystals from pseudostems of banana plants. *RSC Advances* **2014**, *4* (2), 907-915.
50. Mendez, J.; Annamalai, P. K.; Eichhorn, S. J.; Rusli, R.; Rowan, S. J.; Foster, E. J.; Weder, C., Bioinspired mechanically adaptive polymer nanocomposites with water-activated shape-memory effect. *Macromolecules* **2011**, *44* (17), 6827-6835.
51. Shatkin, J. A.; Wegner, T.; Bilek, E. M. T.; Cowie, J., Market projections of cellulose nanomaterial-enabled products- Part 1: Applications. *TAPPI Journal* **2014**, *13* (5), 9-16.
52. Hon, D. N.-S., Cellulose: a random walk along its historical path. *Cellulose* **1994**, *1* (1), 1-25.
53. Zhao, Y.; Zhang, Y.; Lindström, M. E.; Li, J.; Fiber- och, p.; Kth; Skolan för, k., Tunicate cellulose nanocrystals: preparation, neat films and nanocomposite films with glucomannans. *Carbohydrate polymers* **2015**, *117*, 286-296.
54. Nanomaterials; Studies from J.A. Shatkin et al Further Understanding of Nanomaterials (Market projections of cellulose nanomaterial-enabled products - Part 1: Applications). *Nanotechnology Weekly* 2014, p 516.
55. O'Sullivan, A. C., Cellulose: the structure slowly unravels. *Cellulose* **1997**, *4* (3), 173-207.
56. Payen, A., Quatrieme Memoire sur les Developements des Vegetaux, Extrait des Memoires de l'Academie royale des Sciences. *Tome VIII des savants etrangers* **1842**.
57. Staudinger, H.; Fritsch, J., Über Isopren und Kautschuk. 5. Mitteilung. Über die Hydrierung des Kautschuks und über seine Konstitution. *Helvetica Chimica Acta* **1922**, *5* (5), 785-806.
58. González, K.; Retegi, A.; González, A.; Eceiza, A.; Gabilondo, N., Starch and cellulose nanocrystals together into thermoplastic starch bionanocomposites. *Carbohydrate Polymers* **2015**, *117*, 83-90.

59. Kang, H.; Liu, R.; Huang, Y., Graft modification of cellulose: Methods, properties and applications. *Polymer* **2015**, *70*, A1-A16.
60. Crawford, R. J.; Edler, K. J.; Lindhoud, S.; Scott, J. L.; Unali, G., Formation of shear thinning gels from partially oxidised cellulose nanofibrils. *Green chemistry* **2012**, *14* (2), 300-303.
61. Michael, T. P.; András, V.; John, D.; Natalia, F.; Bin, M.; Ryan, W.; Arvind, R.; Robert, J. M.; Ronald, S.; Theodore, H. W.; James, B., Development of the metrology and imaging of cellulose nanocrystals. *Measurement Science and Technology* **2011**, *22* (2), 024005.
62. Agarwal, U. P.; Ralph, S. A.; Baez, C.; Reiner, R. S.; Verrill, S. P., Effect of sample moisture content on XRD-estimated cellulose crystallinity index and crystallite size. *Cellulose* **2017**, *24* (5), 1971-1984.
63. Nageli, C. v., Die Starkekörner. *Pflanzenphysiologische Untersuchungen. vol 1858*, (2).
64. Nishikawa, S., On the spectrum of X-rays obtained by means of lamellar or fibrous substances. *Proceedings of the Tokyo Mathematico-Physical Society. 2nd Series* **1914**, *7* (16), 296-298.
65. Nickerson, R.; Habrle, J., Cellulose intercrystalline structure. *Industrial & Engineering Chemistry* **1947**, *39* (11), 1507-1512.
66. Battista, O. A., Hydrolysis and Crystallization of Cellulose. *Industrial & Engineering Chemistry* **1950**, *42* (3), 502-507.
67. Morehead, F. F., Ultrasonic disintegration of cellulose fibers before and after acid hydrolysis. *Textile Research Journal* **1950**, *20* (8), 549-553.
68. Favier, V.; Canova, G.; Cavallé, J.; Chanzy, H.; Dufresne, A.; Gauthier, C., Nanocomposite materials from latex and cellulose whiskers. *Polymers for Advanced Technologies* **1995**, *6* (5), 351-355.
69. Flauzino Neto, W. P.; Silvério, H. A.; Dantas, N. O.; Pasquini, D., Extraction and characterization of cellulose nanocrystals from agro-industrial residue – Soy hulls. *Industrial Crops and Products* **2013**, *42*, 480-488.
70. Yang, X.; Cranston, E. D., Chemically cross-linked cellulose nanocrystal aerogels with shape recovery and superabsorbent properties. *Chemistry of Materials* **2014**, *26* (20), 6016-6025.
71. Kevin, J.; Yager, K. G.; Hoare, T.; Cranston, E. D., Cooperative ordering and kinetics of cellulose nanocrystal alignment in a magnetic field. *Langmuir* **2016**, *32* (30), 7564-7571.
72. Capadona, J. R.; Shanmuganathan, K.; Tyler, D. J.; Rowan, S. J.; Weder, C., Stimuli-Responsive Polymer Nanocomposites Inspired by the Sea Cucumber Dermis. *Science* **2008**, *319* (5868), 1370-1374.
73. Sacui, I. A.; Nieuwendaal, R. C.; Burnett, D. J.; Stranick, S. J.; Jorfi, M.; Weder, C.; Foster, E. J.; Olsson, R. T.; Gilman, J. W., Comparison of the Properties of Cellulose Nanocrystals and Cellulose Nanofibrils Isolated from Bacteria, Tunicate, and Wood Processed Using Acid, Enzymatic, Mechanical, and Oxidative Methods. *ACS Applied Materials & Interfaces* **2014**, *6* (9), 6127-6138.
74. Santos, R. M. d.; Flauzino Neto, W. P.; Silvério, H. A.; Martins, D. F.; Dantas, N. O.; Pasquini, D., Cellulose nanocrystals from pineapple leaf, a new approach for the reuse of this agro-waste. *Industrial Crops and Products* **2013**, *50*, 707-714.

75. Reid, M. S.; Villalobos, M.; Cranston, E. D., Cellulose nanocrystal interactions probed by thin film swelling to predict dispersibility. *Nanoscale* **2016**, 8 (24), 12247-12257.
76. Hu, Z.; Ballinger, S.; Pelton, R.; Cranston, E. D., Surfactant-enhanced cellulose nanocrystal Pickering emulsions. *Journal of Colloid and Interface Science* **2015**, 439, 139-148.
77. Marchessault, R. H.; Morehead, F. F.; Koch, M. J., Some hydrodynamic properties of neutral suspensions of cellulose crystallites as related to size and shape. *Journal of Colloid Science* **1961**, 16 (4), 327-344.
78. Kalashnikova, I.; Bizot, H.; Cathala, B.; Capron, I., New Pickering Emulsions Stabilized by Bacterial Cellulose Nanocrystals. *Langmuir* **2011**, 27 (12), 7471-7479.
79. Capron, I.; Cathala, B., Surfactant-Free High Internal Phase Emulsions Stabilized by Cellulose Nanocrystals. *Biomacromolecules* **2013**, 14 (2), 291-296.
80. Hu, Z.; Marway, H. S.; Kasem, H.; Pelton, R.; Cranston, E. D., Dried and Redispersible Cellulose Nanocrystal Pickering Emulsions. *ACS Macro Letters* **2016**, 5 (2), 185-189.
81. Kalashnikova, I.; Bizot, H.; Bertoncini, P.; Cathala, B.; Capron, I., Cellulosic nanorods of various aspect ratios for oil in water Pickering emulsions. *Soft Matter* **2013**, 9 (3), 952-959.
82. Tang, J.; Lee, M. F. X.; Zhang, W.; Zhao, B.; Berry, R. M.; Tam, K. C., Dual Responsive Pickering Emulsion Stabilized by Poly[2-(dimethylamino)ethyl methacrylate] Grafted Cellulose Nanocrystals. *Biomacromolecules* **2014**, 15 (8), 3052-3060.
83. Kosonen, M. V.; Rätty, M.; Ventola, J., Method for making paper product and paper product. Google Patents: 2013.
84. Xu, X.; Liu, F.; Jiang, L.; Zhu, J. Y.; Haagenson, D.; Wiesenborn, D. P., Cellulose Nanocrystals vs. Cellulose Nanofibrils: A Comparative Study on Their Microstructures and Effects as Polymer Reinforcing Agents. *ACS Applied Materials & Interfaces* **2013**, 5 (8), 2999-3009.
85. Quennouz, N.; Hashmi, S. M.; Choi, H. S.; Kim, J. W.; Osuji, C. O., Rheology of cellulose nanofibrils in the presence of surfactants. *Soft Matter* **2016**, 12 (1), 157-164.
86. Turbak, A. F.; Snyder, F. W.; Sandberg, K. R., *Microfibrillated cellulose, a new cellulose product: properties, uses, and commercial potential.*; ITT Rayonier Inc., Shelton, WA: 1983; p Medium: X; Size: Pages: 815-827.
87. Ougiya, H.; Watanabe, K.; Morinaga, Y.; Yoshinaga, F., Emulsion-stabilizing Effect of Bacterial Cellulose. *Bioscience, Biotechnology, and Biochemistry* **1997**, 61 (9), 1541-1545.
88. Cranston, E., Transforming Nanocellulose into Sustainable Products through Surface Engineering. In *9th Annual Chemical Engineering Research Symposium*, Virginia Tech, 2017.
89. Peng, B. L.; Dhar, N.; Liu, H. L.; Tam, K. C., Chemistry and applications of nanocrystalline cellulose and its derivatives: A nanotechnology perspective. *The Canadian Journal of Chemical Engineering* **2011**, 89 (5), 1191-1206.
90. Cowie, J.; Bilek, E.; Wegner, T.; Shatkin, J. A., Market projections of cellulose nanomaterial-enabled products-- Part 2: Volume estimates. *TAPPI Journal* **2014**, 13 (6), 57-69.

## **Chapter 2: Problem Statement and Objective**

The goal of this thesis is to develop an alternate feedstock for cellulose nanocrystals (CNCs) and to investigate their use in a water-actuating smart composite. The bulk of the thesis focused on the use of CNCs as a reinforcement agent for thermoplastic polyurethane (TPU). CNCs were chosen due to their unique combination of mechanical properties and environmentally friendly production when compared to many other materials. There is a growing field of research in finding uses for CNCs that has been very fruitful. TPU was chosen because of its mechanical properties, ease of working with, ease of procuring, and a high level of working knowledge by the authors. TPU is also a very common polymer that is used in many environments.

The goal of isolating CNCs from pistachio shells is to find an upscaling use for what is currently a waste product. This would allow farmers to add value to their operations as well as provide bio-refineries another feedstock for CNC production. Pistachio shells were chosen for this because they are a waste product and because of their light weight, high strength, and high stiffness, which are all indicative of CNCs. Our hope is that introducing more agricultural waste into the supply chain of CNCs will help to drive the cost of production down so that more applications for CNCs will become economically feasible. Despite the large volume of literature on alternate feedstocks, there has not, to my knowledge, been any research investigating the use of pistachio shells. Chapter 3 outlines research on this isolation and includes a procedure for purifying the cellulose, isolating the CNCs, and using them in TPU matrix composites to show an increase in stiffness. We found that our method of isolation of CNCs from

pistachio shell had a relatively high yield compared to other agro wastes, and the isolated CNCs had high aspect ratios, relatively low crystallinity, and low charge ratios.

Chapter 4 discusses work done to create water-actuating films based on CNC-based composites. The chosen matrix polymer was TPU because it has a low glass transition temperature, low Young's modulus, and very low adsorption of water. CNCs were chosen as the additive because of their rapid uptake of water and environmental sustainability. Characterization was done to determine the degree of swelling and Young's modulus of the CNC/TPU composites at several different concentrations so that the system could be accurately modeled. Several methods of potentially producing such films were also explored.

## **Chapter 3: The Isolation of Cellulose Nanocrystals from Pistachio Shells Via Acid Hydrolysis.**

### **3.1 Abstract**

The pistachio nut (*Pistacia vera*) is a common food source. The shell of the nut has few known applications and is considered a waste product of the agriculture industry (agro waste). In this paper, we show a method for isolating cellulose nanocrystals (CNCs) from the pistachio shell. CNCs are well known for having very good mechanical properties which have shown themselves to be effective in many different polymer based nanocomposites. We show that common methods of purifying and hydrolyzing cellulose will result in useable CNCs. We found a yield of  $15\pm 14$  wt %, which is higher than other agro waste products. We found an aspect ratio of  $17\pm 3$ , a crystallinity of 66%, and a surface charge density of  $90\pm 12$  mmol/kg. These numbers compare well with other common commercial sources of CNCs.

### **3.2 Introduction**

Cellulose is the most abundant bio-polymer in the world with an estimated  $10^{10}$  to  $10^{12}$  tons produced annually.<sup>1</sup> The structure of cellulose is a chain of pyranose rings connected through 1-4  $\beta$  bonds.<sup>2</sup> The cellulose molecule has two strong hydrogen bonding sites off of the two hydroxyl groups which allow for it to achieve crystal structures.<sup>2</sup> There are four crystal structures for cellulose, but cellulose I and cellulose II are the most common with cellulose III and IV being less stable derivatives of I and II.<sup>2</sup> Cellulose is a primary constituent of lignocellulose which includes cellulose, lignin and hemicellulose.<sup>2-4</sup> Lignocellulose is found in the cell walls of plants and provides the



physical strength of the plant.<sup>2-4</sup> The structure of lignocellulose has roughly square cellulose fibrils connected to lignin fibers by hemicellulose.<sup>2,4</sup>

First identified in the 1950s, cellulose nanocrystals (CNCs) are a crystalline form of cellulose which exist in plant matter surrounded by amorphous cellulose.<sup>4-5</sup> CNCs have been under increased investigation due to their sustainability and mechanical properties.<sup>3-4,6</sup> It has been noted that, despite all being of the same chemistry, the physical dimensions of the CNCs and some mechanical properties can change drastically based on the source of the cellulose.<sup>5</sup> These properties are also dependent on the process used to isolate them from the bulk cellulose.<sup>5</sup>

To remove the CNCs from the cellulose, a variety of acids have been employed with the main ones being sulfuric acid, hydrochloric acid, and phosphoric acid.<sup>3,6-7</sup> Other acids have also been proven to be effective in different yield amounts and different surface charges, small molecules which attach to the surface.<sup>3,8</sup> The resulting crystals are rod-like in shape, they are between 100 nm and 1000 nm long, and they have an aspect ratio of between 10 and 67.<sup>3</sup> The crystals are of interest primarily for their physical and mechanical properties, including high stiffness, strength, and aspect ratio.<sup>3,6</sup> These properties make CNCs an excellent option for use as reinforcement in various polymer nanocomposites including polyethylene, polyester, and polyurethane.<sup>3-4,9-11</sup> Also, the surface of CNCs can be easily modified<sup>5-6</sup> for use in stimuli responsive materials<sup>12-14</sup>, electronic materials<sup>15</sup>, and optical materials<sup>16</sup>.

The usefulness of cellulose nanocrystals has already created a small market.<sup>17</sup> This market is expected to increase in size from 120 metric tons in 2013 to 770 metric tons per year in 2017 by increasing the number industries which use CNCs in high-end

products.<sup>1, 17-18</sup> Eventually, CNCs will hopefully be included in large-scale manufacturing of nanocomposites for more moderately priced goods like concrete and paper products.<sup>1</sup>

In order to increase the marketability of CNCs, this report looks at the use of an agricultural waste product, the shell of *Pistacia vera* (pistachio shells), as a feedstock for their extraction. To the best of our knowledge, pistachio shells have not been investigated as a source for CNC isolation. We chose this material due to its seemingly high rigidity and high strength and because it is an agricultural waste product. The reason that we were specifically looking at a waste product is because there is already significant infrastructure in place for the growth and removal of the product with nearly 1 million tons of pistachios produced annually for consumption of the nut. {Sorrenti, 2016 #131}. The shells make up between 40 and 50 percent of the nut, so it is estimated that between 400,00 and 500,000 tons of pistachio shells are produced globally every year. {Açıklalın, 2012 #161} There is little other use for pistachio shells that we would be competing with, meaning that the pistachio shells would be a low cost feedstock with minimal startup cost.<sup>19-20</sup> It is the hope of the authors that adding pistachio shells as a low-cost source of CNCs will lead to an increase in cellulose nanocrystal production as well as a reduction in production cost. With this goal in mind, we give a protocol for using sulfuric acid-based hydrolysis was used to isolate the nanocrystals. The procedure is based on Muller et al's procedure for isolating CNCs from the pseudostems of banana plants.<sup>6</sup>

### **3.3. Procedure and Materials**

#### **3.3.1 Materials**

Sodium hydroxide pellets were purchased from Sigma Aldrich. Glacial acetic acid and ACS reagent grade sulfuric acid were purchased from Spectrum Chemical. Raw pistachios were purchased from CVS Pharmacy and the shells were removed for use. McKesson brand topical hydrogen peroxide solution was purchased via Amazon. GE Whatman filter paper was used in the filtration. All water was filtered in the lab before use. Fisherbrand cellulose extraction thimbles were purchased from Fischer Scientific. Nanovan, a suspension of vanadium particles in water, was purchased from Nanoprobes. Bovine serum albumin (BSA), dichloromethane (DCM), and dimethyl sulfoxide (DMSO) was purchased from Sigma Aldrich. Texin RxT70A thermoplastic polyurethane (referred to as TPU) was received from Covestro. Commercially available wood based CNCs were purchased from the University of Maine Nanocellulose Facility. Ethanol and toluene were purchased from the Department of Chemistry at Virginia Tech.

### **3.3.2 Collecting and milling the shells**

The pistachio shells were washed, dried, and milled using a Spex 8000 mixer mill using stainless steel balls and a charge ratio, the ratio of the mass of milling media to the mass of shells, of 8 for 30 minutes. The result was a fine powder that was characterized by XRD and then used in the next steps.

### **3.3.3 Purification and bleaching of cellulose**

The extraction and bleaching procedure was adapted from Mueller et al. and is similar to other bleaching procedures. {Mueller, 2014 #12}{Santos, 2013 #42}{Silvério, 2013 #71} Approximately 10 grams of pistachio shell powder was measured out and purified in a soxhlet extractor using 1000 ml of 1/3 ethanol and 2/3 toluene by volume to

remove monomers such as sugars. After 24 hours, the thimble was removed and left to dry overnight.

The hemicellulose was removed via repeated base washes. For each wash, a 1 M sodium hydroxide solution was created by mixing 40 g of sodium hydroxide pellets with 1000 mL of water and heated to 70 °C while stirring constantly for 30 minutes. The extracted cellulose was added to the solution for 2 hours before it was separated via vacuum filtration. The cellulose was then washed with another 1000 mL of fresh water. This process was repeated until the water was clear, about 6 times.

The lignin was removed via repeated hydrogen peroxide solution washes. A hydrogen peroxide and acetic acid solution was created by mixing approximately 440 mL of 3% hydrogen peroxide and 1 mL of acetic acid to 560 mL of water (1.3 v/v hydrogen peroxide and 0.1 v/v acetic acid). This mixture was heated to 60 °C and stirred constantly for 30 minutes before the cellulose was added. The cellulose was filtered out of that bath after 2 hours and was washed with another 1000 mL of water. This process was repeated until the cellulose became an off-white mass and did not change colors, about 6 times.

Once these baths were done, a final soxhlet extraction, with the same parameters as above, was used to remove any excess chemicals or particles. The cellulose was then pure and was used without any characterization.

#### **3.3.4 Hydrolysis of cellulose**

Three grams of the purified cellulose was placed in 250 mL of water and cooled in a refrigerator set to 5°C overnight. The following day, it was put into an ice bath as 150 mL of sulfuric acid was added dropwise, keeping the temperature below 20 °C. Once all of the acid had been added, the temperature was increased to 50 °C for 90 minutes.

After that, the acid was removed by centrifuging at 10000 rpm and decanting the supernatant until the pH was neutral (around 4 times). Following that, the cellulose was dialyzed against water for 3 days, replacing the water daily. The cellulose mass was then sonicated for 30 minutes and lyophilized. The resulting powder was then weighed to determine yield by comparing to the weight of the purified cellulose.

### **3.3.5 Microscopy**

#### **3.3.5.1 Scanning Electron Microscopy**

Samples were dispersed in water with 1 mg being dispersed in 10 mL of water and 42.1 mg of BSA and sonicated for 10 hours, adding ice to the bath regularly to control the temperature. After sonication, a drop of the mixture was placed on an aluminum stand and left to dry overnight. The next day, a drop of NanoVan<sup>®</sup> was added onto the sample and left for 30 seconds before being wicked away. The stands were sputter coated with 4 nm of iridium to prevent charging and imaged in LEO 1550 field-emission SEM (FE-SEM) using 5 kV.

#### **3.3.5.2 Transmission Electron Microscopy**

Like SEM, TEM samples were made by dispersing 1 mg of CNCs in 10 ml of water. 42.1 mg of BSA were added to the solution, followed by 10 hours of sonication in a bath sonicator, again using ice to control the temperature. A drop of the liquid was placed on a TEM grid and left to dry. After one minute, a drop of NanoVan<sup>®</sup> was added to the CNC mixture on the TEM grid for 30 seconds. Excess solution was washed away by placing the grid in water for a very short period of time. Imaging was done on a JEOL 2100 TEM.

### 3.3.6 X-Ray Diffraction

X-ray diffraction was performed using a Panalytical X'Pert powder x-ray diffraction system using a CuK $\alpha$  radiation source, a tension of 45 kV and a current of 30 mA. Measurements were taken from 0 to 50 degrees. The peak height ratio method of determining the percent crystallinity was used utilizing equation.1<sup>21</sup>

$$\% \text{crystallinity} = \frac{(I_{200} - I_{am})}{I_{200}}$$

Equation 3.1: Finding the percent crystallinity of a polymer from XRD.

$I_{200}$ : 200 peak intensity found at 22 degrees,  $I_{am}$ : amorphous intensity found at 18 degrees

### 3.3.7 Charge Density

The charge density was found through charge titration using a previously proven method.<sup>7</sup> 50 mg of CNCs were added to 200 mL of water. 20 mL of 0.01 M HCl was added to the water. The pH and conductivity of the solution were both measured incrementally as 0.01 M NaOH was added. The concentration was calculated using equation 3.2 below. The volume used in the equation is the volume where the solution is actively buffering. Measurements were done on a Thermo Scientific Orion Star A215 pH/Conductivity meter.

$$\frac{(C_{NaOH} * V_{NaOH})}{W_{CNCs}} * 10^6 = \frac{\text{mmol SO}_4}{\text{kg cellulose}}$$

Equation 3.2: Calculates charge density of CNCs

$C_{NaOH}$ : molarity of NaOH solution,  $V_{NaOH}$ : volume of NaOH buffered,  $W_{CNCs}$ : mass of CNCs

### 3.3.8 Dispersibility

We tested to see how well the synthesized CNCs were dispersed in a series of solvents, including water, dimethylformamide (DMF), dichloromethane (DCM),

dimethyl sulfoxide (DMSO), ethanol, and toluene. 0.04 g of CNCs were added to 20 mL of each solvent in a vial, and the solutions were sonicated in a bath sonicator for 8 hours. Once they were dispersed, they were set aside and had pictures taken of them at 0, 12, and 24 hours. After ten days, TEM samples were created using the method discussed in 2.5.2.

### **3.3.9 Mechanical Reinforcement**

CNC composites were made by solvent casting different samples: TPU reinforced with pistachio-based CNCs, commercially available CNCs derived from wood, and unmodified polyurethane. To make these, the TPU was dissolved in DMF in a ratio of 50 mg/ml. Likewise, CNCs were dispersed in DMF using a ratio of 0.04 g in 20 mL and sonicated for 8 hours in a bath sonicator. The polyurethane was reinforced with 5 wt% CNCs, using 14.4 mL of the TPU solution and all of the CNC dispersion. The mixtures were cast in Teflon dishes at 80 °C overnight.

The composites were cut using a dog bone die on a manual press. The gauge length was 7 mm, and the width was 3 mm. A TA Q800 dynamic mechanical analyzer (DMA) was used under controlled force using a film tension camp. The force was ramped at a rate of 0.5 N/min to find the modulus of elasticity and yield stress.

## **3.4 Results and Discussion**

### **3.4.1 Purification of Cellulose**

The material used for this procedure was the hard outer shell of the shell of the *pistacia vera*. Following the steps reported for extracting and bleaching cellulose for banana pseudostems<sup>6</sup> yielded an off-white solid mass that resembled paper. These

procedures removed the lignin, hemicellulose, and extractives, leaving cellulose as the product.

### 3.4.2 Hydrolysis

After hydrolysis and lyophilization, the hydrolyzed pulp existed as a tan powder. The average yield of the hydrolyzed cellulose was  $50 \pm 15$  percent of the cleaned cellulose. For other agro-waste products, yields have been shown between 5 percent for rice straw and 77 percent for pineapple leaf, with most sources appearing to be between 20 and 30 percent.<sup>6, 22-25</sup> The high yield is important in creating an industrially viable source of nanocrystals. Figure 3.1 on the next page shows pictures of the shells at various stages of the process.



Figure 3.1a: Pistachio in the shell. b: Milled shell. c: Post extraction cellulose. d: Dried CNCs.

### 3.4.3 Microscopy

FE-SEM and TEM were both used to observe the morphology.

#### 3.4.3.1 Scanning Electron Microscopy

The FE-SEM images (figure 3.2) show the CNCs to be cylindrical, as was expected. There were a few small unknown particles still present after the cleaning and hydrolysis procedures which we believe to be dust or other contaminants.



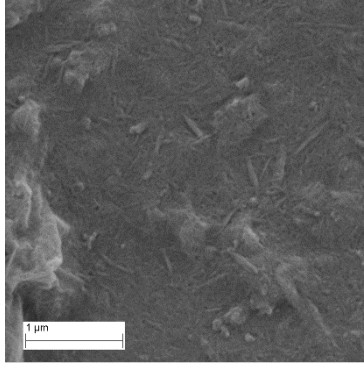


Figure 3.2: SEM image of isolated CNCs

### 3.4.3.2 Transmission Electron Microscopy

Transmission electron microscopy was also used to observe morphology and aspect ratio (figure 3.3). The morphology appeared to be cylindrical as expected and observed by SEM. Using Klonk Image Measurement software, the CNCs were measured to be  $187\text{nm} \pm 42\text{ nm}$  long and  $12\text{nm} \pm 1\text{ nm}$  wide with a high aspect ratio,  $16 \pm 3$ .

These numbers compare well with other sources which have aspect ratios from 4 to 13.<sup>6,</sup>

<sup>22</sup> The higher aspect ratio is very helpful in creating a strong composite material as it increases the interface area, allowing more load to be transferred to the fiber.

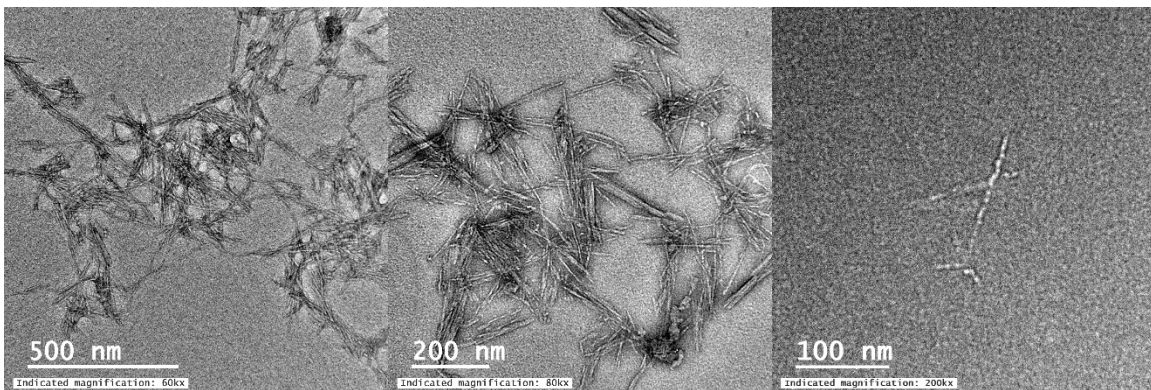


Figure 3.3: TEM of isolated CNCs

### 3.4.4 X-Ray Diffraction

Small angle x-ray diffraction showed a removal of most of the amorphous material (figure 3.4). The peaks appeared to be at a  $2\theta$  of  $14.5^\circ$ ,  $16.6^\circ$ ,  $22.5^\circ$ , and  $34.4^\circ$  which line up with the  $1\bar{1}0$ ,  $110$ ,  $200$ , and  $004$  planes respectively.<sup>21,23</sup> These spectra

indicated that the cellulose is in the form of cellulose I.<sup>21</sup> The calculated percent crystallinity is 67% using the peak height method discussed in section 3.3.6. The total crystallinity is within the expected range for CNCs, though it is on the lower end of the spectrum. The range of crystallinities in literature ranges from 64 percent to 91 percent in the literature with many reporting a cluster in the mid to upper 70s.<sup>6, 23-24</sup> High crystallinity is one of the primary factors in reinforcement of polymer nanocomposites as the crystallinity is responsible for much of the high stiffness.

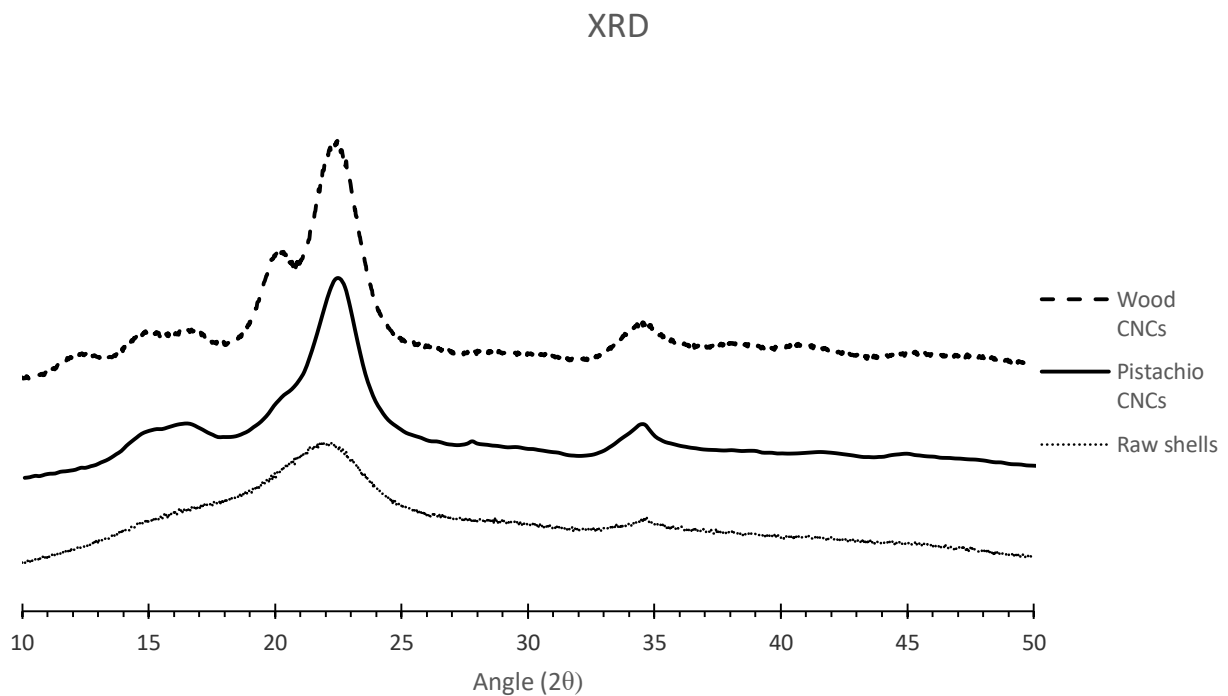


Figure 3.4: XRD spectra comparing crystallinity of pistachio shells, CNCs isolated from the pistachio shells, as well as commercially available CNCs for comparison.

### 3.4.5 Surface Titration

CNCs produced via acid hydrolysis often have sulfate groups attached to them. By doing the surface titration, we can see how many hydroxyl groups became sulfate half esters. The amount of sulfate groups was found using the procedure in 3.3.7 By plotting the conductivity against volume of base, there is an obvious buffered region. By

observing the length of the buffered region, the number of moles of sulfate groups can be found using the equation from section 3.3.7, it was determined that the concentration is  $90 \pm 12$  mmol/kg. The charges help the cellulose to be easily dispersed in polar solvents, such as water, but also lower the onset of thermal degradation.<sup>3,7</sup> This compares favorably with other sources which cluster slightly above 100 mmol/kg.<sup>6,24</sup>

### 3.4.6 Dispersibility

Figure 3.5 below shows the pictures of the different solvents over the course of several days. There was not noticeable change after one day. The results were confirmed through observing the density of CNC aggregates. Through this, we confirmed that DMF was held the CNCs in suspension for the longest, with water and DMSO being a good alternative for short periods of time. DCM, ethanol, and toluene were all poor choices for dispersing. This result was expected and seen across many CNCs.<sup>6</sup> The reason for the quick precipitation of CNCs is because they have been dried and re-dispersed which has been shown to reduce the time in dispersion without the addition of sodium. {Beck, 2012 #163}

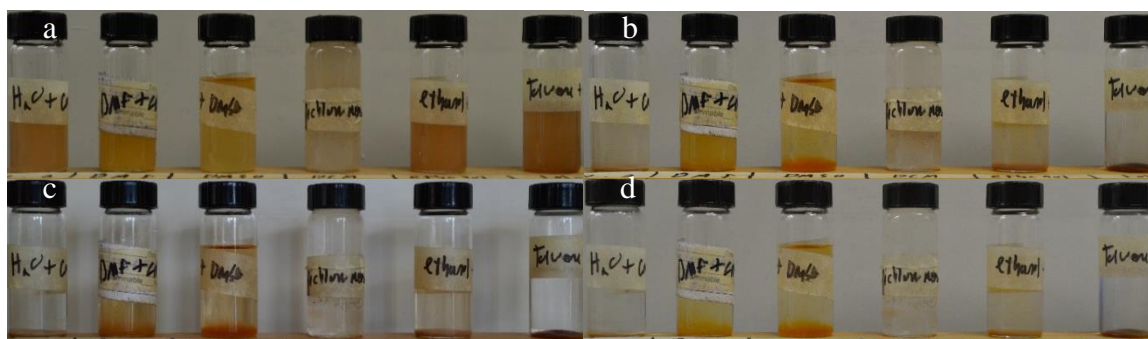


Figure 3.5: Dispersibility of CNCs after a) 0 hours, b) 0.5 hours, c) 12 hours, and d) 24 hours in water, DMF, DMSO, DCM, ethanol, and toluene.

### 3.4.7 Mechanical Testing

We saw a significant increase in the modulus of elasticity in the CNC-TPU composite samples and yield stress. The modulus of elasticity went up from  $2.32 \pm 0.53$  to  $4.58 \pm 0.97$  MPa with the addition of 5 wt% CNCs isolated from pistachio shells. The yield stress was found to have increased from  $0.80 \pm 0.29$  to  $1.50 \pm 0.34$  MPa. We have been able to show how the addition of CNCs from pistachio shell can reinforce, but the effect is lesser than that of the composites made with commercially available CNCs, which had a modulus of elasticity of  $16.28 \pm 8.2$  MPa and a yield stress of  $2.2 \pm 0.6$  MPa. We believe that the low crystallinity index of the isolated nanocrystals is the primary reason that the reinforcement fell short of the commercial CNCs.<sup>26</sup> Figure 3.6 on the next page shows a plot of the stress versus strain of the pure TPU, as well as TPU reinforced with 5wt% of pistachio shells and TPU reinforced with 5wt% commercial CNCs.

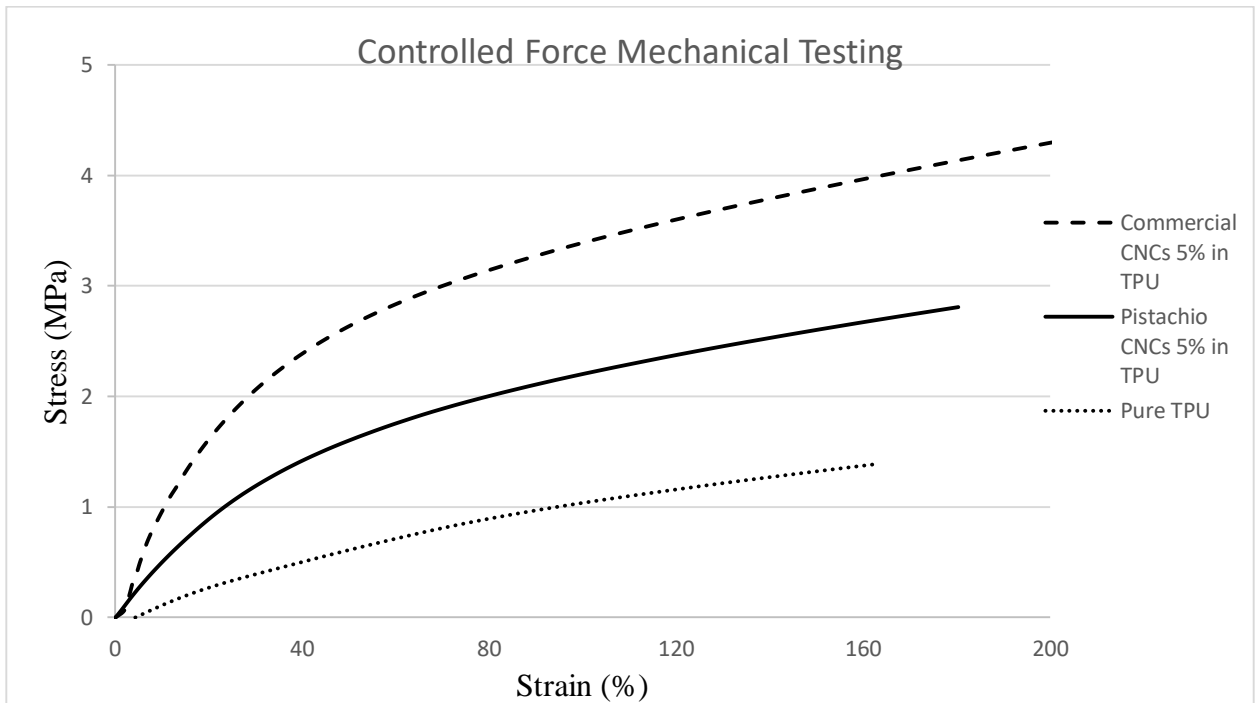


Figure 3.6: Stress-strain plots showing pure TPU, TPU reinforced with either CNCs isolated from pistachio shells or commercially available CNCs isolated from wood.

### **3.5. Conclusion**

We have proven that pistachio shells offer a high-yield feedstock material for the isolation of cellulose nanocrystals. We were able to use common methods to purify the cellulose from the shell and sulfuric acid hydrolysis to isolate the CNCs from the amorphous cellulose. The yield of CNCs was  $50 \pm 14$  percent of the pure cellulose with an aspect ratio of  $12 \pm 7$ . An apparent crystallinity of 66 percent was observed as well as a charge density of  $102 \pm 10$  mmol/kg. We also observed the dispersibility of CNCs in several solvents. Finally, we compared the mechanical behaviors of composites made with pistachio shell-based CNCs with composites made with commercially available wood-based CNCs. The produced nanocrystals compared well with other nanocrystals, showing that pistachio shells are viable as an alternate feedstock, which is especially important as they are a large waste product which is grown and discarded all over the world.<sup>19-20</sup>

### **Acknowledgements**

The authors would like to thank the Materials Science and Engineering Department at the Virginia Polytechnic Institute and State University for use of their equipment, including the Panalitical XRD and the TA Q800 DMA. We would also like to thank Hesham Elmkharram for his help in training me on the use of the high-energy ball mill and the Panalitical XRD. We would like to thank Kelly Stinson-Bagby for her help with the surface titration and running the TEM. We would like to acknowledge Steve McCartney for his help with the SEM. This research did not receive any specific grant from funding agencies in the public, commercial, or not-for-profit sectors.

### **3.6 References**

1. Shatkin, J. A.; Wegner, T.; Bilek, E. M. T.; Cowie, J., Market projections of cellulose nanomaterial-enabled products- Part 1: Applications. *TAPPI Journal* **2014**, *13* (5), 9-16.
2. O'Sullivan, A. C., Cellulose: the structure slowly unravels. *Cellulose* **1997**, *4* (3), 173-207.
3. Dufresne, A., *Nanocellulose: from nature to high performance tailored materials*. De Gruyter: Berlin;Boston, 2012; Vol. 1. Aufl.
4. Moon, R. J.; Martini, A.; Nairn, J.; Simonsen, J.; Youngblood, J., Cellulose nanomaterials review: structure, properties and nanocomposites. *Chemical Society reviews* **2011**, *4* (7), 3941-3994.
5. Habibi, Y.; Lucia, L. A.; Rojas, O. J., Cellulose Nanocrystals: Chemistry, Self-Assembly, and Applications. *Chemical Reviews* **2010**, *110* (6), 3479-3500.
6. Mueller, S.; Weder, C.; Foster, E. J., Isolation of cellulose nanocrystals from pseudostems of banana plants. *RSC Advances* **2014**, *4* (2), 907-915.
7. Espinosa, S. C.; Kuhnt, T.; Foster, E.; Weder, C., Isolation of Thermally Stable Cellulose Nanocrystals by Phosphoric Acid Hydrolysis. *Biomacromolecules* **2013**, *14* (4), 1223-1230.
8. Lu, Q.; Cai, Z.; Lin, F.; Tang, L.; Wang, S.; Huang, B., Extraction of Cellulose Nanocrystals with a High Yield of 88% by Simultaneous Mechanochemical Activation and Phosphotungstic Acid Hydrolysis. *ACS Sustainable Chemistry & Engineering* **2016**, *4* (4), 2165-2172.
9. Kargarzadeh, H.; M. Sheltami, R.; Ahmad, I.; Abdullah, I.; Dufresne, A., Cellulose nanocrystal: A promising toughening agent for unsaturated polyester nanocomposite. *Polymer* **2015**, *56*, 346-357.
10. Sapkota, J.; Jorfi, M.; Weder, C.; Foster, E. J., Reinforcing Poly(ethylene) with Cellulose Nanocrystals. *Macromolecular Rapid Communications* **2014**, *35* (20), 1747-1753.
11. Pei, A.; Malho, J.-M.; Ruokolainen, J.; Zhou, Q.; Berglund, L. A., Strong Nanocomposite Reinforcement Effects in Polyurethane Elastomer with Low Volume Fraction of Cellulose Nanocrystals. *Macromolecules* **2011**, *44* (11), 4422-4427.
12. Annamalai, P. K.; Dagnon, K. L.; Monemian, S.; Foster, E. J.; Rowan, S. J.; Weder, C., Water-Responsive Mechanically Adaptive Nanocomposites Based on Styrene-Butadiene Rubber and Cellulose Nanocrystals—Processing Matters. *ACS Applied Materials & Interfaces* **2014**, *6* (2), 967-976.
13. Zhao, L.; Li, W.; Plog, A.; Xu, Y.; Buntkowsky, G.; Gutmann, T.; Zhang, K., Multi-responsive cellulose nanocrystal-rhodamine conjugates: an advanced structure study by solid-state dynamic nuclear polarization (DNP) NMR. *Physical Chemistry Chemical Physics* **2014**, *16* (47), 26322-26329.
14. Abdollahi, A.; Rad, J. K.; Mahdavian, A. R., Stimuli-responsive cellulose modified by epoxy-functionalized polymer nanoparticles with photochromic and solvatochromic properties. *Carbohydrate Polymers* **2016**, *150*, 131-138.
15. Wu, X.; Tang, J.; Duan, Y.; Yu, A.; Berry, R. M.; Tam, K. C., Conductive cellulose nanocrystals with high cycling stability for supercapacitor applications. *Journal of Materials Chemistry A* **2014**, *2* (45), 19268-19274.
16. Zhang, Y. P.; Chodavarapu, V. P.; Kirk, A. G.; Andrews, M. P., Nanocrystalline cellulose for covert optical encryption. *NANOP* **2012**, *6* (1), 063516-1-063516-9.

17. Inc, F. M., The Global Market for Nanocellulose to 2014. *Technology Report* **2012**, 60.
18. Cowie, J.; Bilek, E.; Wegner, T.; Shatkin, J. A., Market projections of cellulose nanomaterial-enabled products-- Part 2: Volume estimates. *TAPPI Journal* **2014**, 13 (6), 57-69.
19. Sorrenti, S., Non-wood forest products in international statistical systems. **2016**.
20. Komnitsas, K.; Zaharaki, D.; Pyliotis, I.; Vamvuka, D.; Bartzas, G., Assessment of Pistachio Shell Biochar Quality and Its Potential for Adsorption of Heavy Metals. *Waste and Biomass Valorization* **2015**, 6 (5), 805-816.
21. Thygesen, A.; Oddershede, J.; Lilholt, H.; Thomsen, A. B.; Ståhl, K., On the determination of crystallinity and cellulose content in plant fibres. *Cellulose* **2005**, 12 (6), 563.
22. Santos, R. M. d.; Flauzino Neto, W. P.; Silvério, H. A.; Martins, D. F.; Dantas, N. O.; Pasquini, D., Cellulose nanocrystals from pineapple leaf, a new approach for the reuse of this agro-waste. *Industrial Crops and Products* **2013**, 50, 707-714.
23. Lu, P.; Hsieh, Y.-L., Preparation and characterization of cellulose nanocrystals from rice straw. *Carbohydrate Polymers* **2012**, 87 (1), 564-573.
24. Flauzino Neto, W. P.; Silvério, H. A.; Dantas, N. O.; Pasquini, D., Extraction and characterization of cellulose nanocrystals from agro-industrial residue – Soy hulls. *Industrial Crops and Products* **2013**, 42, 480-488.
25. Sheltami, R. M.; Abdullah, I.; Ahmad, I.; Dufresne, A.; Kargarzadeh, H., Extraction of cellulose nanocrystals from mengkuang leaves (*Pandanus tectorius*). *Carbohydrate Polymers* **2012**, 88 (2), 772-779.
26. Silvério, H. A.; Neto, W. P. F.; Dantas, N. O.; Pasquini, D., Extraction and characterization of cellulose nanocrystals from corncob for application as reinforcing agent in nanocomposites. *Industrial Crops and Products* **2013**, 44, 427-436.

## **Chapter 4: Creating a Water Activated, Self-folding Film from Cellulose Nanocrystals and Polyurethane.**

### **4.1 Abstract**

Self-folding materials are under increased investigation due to their ability to create precise motion without the need of large external motors. We report a potential method of using a functionally-graded composite material using thermoplastic polyurethane (TPU) reinforced with cellulose nanocrystals (CNCs) to create a film that can reversibly actuate when exposed to water. This material utilizes the different swelling behaviors of CNC-rich TPU and pure TPU. The created films are predicted to be able to bend up to 0.35 times the length of the actuating area, depending on the concentration of CNCs and thickness of the film.

### **4.2 Introduction**

Recently, there has been a lot of interesting research done in self-folding materials. Using 3D printing techniques on self-folding materials to create parts that later shape into a final part is often called 4D printing. Heat<sup>1</sup>, light<sup>2-3</sup>, electrical current<sup>4</sup>, and swelling behaviors<sup>5</sup> have already been shown to create movement in 4D printing. These unique self-moving materials enable new functionality for existing applications including creating self-folding furniture,<sup>6</sup> pump-less plumbing systems,<sup>7</sup> smart valves,<sup>8</sup> packing systems,<sup>9</sup> and even robots<sup>10</sup>.

Self-folding materials can be used to create compact structures by using techniques derived from the art of origami.<sup>11</sup> They have also used specific folding techniques to create movement using very little space.<sup>10,12</sup> Uses for these machines include surgical tools,<sup>13</sup> solar panel arrays,<sup>9</sup> release mechanisms,<sup>14</sup> and robot



construction<sup>10</sup>. The benefits of these devices are their ability to move between a flat geometry (deployed) and a complicated 3D structure (folded) while keeping the part as simple and as small as possible.<sup>9, 11, 13-14</sup>

The most common self-folding structures are composite materials bound by a single joint where each material has a different coefficient of thermal expansion.<sup>15</sup> A structure's degree of actuation is determined by the difference in elongation, causing internal stresses which bend the film. These cantilever systems are commonly used in small electronic devices as a method of monitoring temperature<sup>16-19</sup> or to manipulate objects<sup>15, 19</sup>. This type of self-folding material is easily modeled by equation 1 below where  $\kappa$  is the curvature, E is the elastic modulus, h and H are the heights of the deposited material and substrate, and  $\Delta\epsilon$  is the change in strain.<sup>20</sup> This equation is general enough to be used for any bilayer bending film.<sup>20</sup>

$$\kappa = \frac{6 E_d E_s (h + H) h H \Delta\epsilon}{E_d^2 h^4 + 4 E_d E_s h^3 H + 6 E_d E_s h^2 H^2 + 4 E_d E_s h H^3 + E_s^2 H^4}$$

Equation 4.1: finding the curvature of a bi-metallic strip.<sup>20</sup>

Other common mechanisms for self-folding include the use of two materials with different swelling behaviors.<sup>5, 8, 21-22</sup> This mechanism is similar to the thermally activated structures; however, the stress is produced by a difference in swelling in water or other liquid. There are numerous applications for such a film, including self-assembling as discussed above,<sup>21</sup> shape memory,<sup>23</sup> smart valves,<sup>8</sup> and detection of different solvents<sup>5</sup>. Another possible model for actuation of swelling-based materials is given as equation 2.<sup>21</sup> This equation was created using poly(ethylene glycol methacralate) blended with

poly(ethylene glycol dimethacrylate) as the swelling layer and chitosan as the non-swelling layer.<sup>21</sup>

$$y_{max} = \frac{3 \left( v_b^{\frac{1}{3}} - 1 \right) \left[ \frac{t_a v_a}{t_a + t_b} + \frac{t_b v_b}{t_a + t_b} - 1 \right] (t_a + t_b)^2}{(v_b - 1) t_b^2 * \left[ 4 + 6 * \frac{t_a}{t_b} + 4 * \frac{t_a^2}{t_b^2} + \frac{E_a t_a^3}{E_b t_b^3} + \frac{E_b t_b}{E_a t_a} \right]}$$

Equation 4.2: finding the maximum bending of swelling based composites.<sup>21</sup>  $t$  is the thickness of each layer,  $v$  is the volume swelling ratio, and  $E$  is the elastic modulus.

Cellulose nanocrystals (CNCs) have several unique properties, such as their swelling mechanics, which have recently been of particular interest.<sup>23-24</sup> CNCs have two very useful properties for creating a self-folding material. They increase the Young's modulus when dry and reduce it when wet, and they have aligned hydrogen bond sites, which allow for higher levels of swelling.<sup>23, 25-26</sup> We report what I believe could be a method to create a bilayer film which bends due to a difference in swelling behaviors created by a functional gradient of concentration of CNCs in thermoplastic polyurethane.

### 4.3 Materials

N-N Dimethylformamide (DMF) and phosphoric acid were purchased from Sigma Aldrich. Elastollan Soft 35 thermoplastic polyurethane was obtained from BASF. Texin RxT70A thermoplastic polyurethane was obtained from Covestro. DI water was filtered in the lab. Commercially available wood-based cellulose nanocrystals (CNCs) were purchased from the University of Maine Nanocellulose Facility. Whatman filter paper was purchased from Fisher Scientific.

#### 4.4.1 Preparing pressed films

First, films of CNCs in Texin were created by solution casting. The Texin was dissolved in DMF at a concentration of 50 mg/mL. CNCs were dispersed in DMF at

various concentrations and sonicated for 2 hours to remove aggregates. Films were then cast by combining the CNC dispersion with the Texin mixture at a concentration of 10, 20, 30, 60, 90 wt% CNC. The films were cast in a vacuum oven at 80 °C overnight. Similarly, films were cast out of pure Texin TPU. The pure polyurethane films were clear and flexible, while the films that included CNCs were cloudy and were notably stiffer, as expected.

Once the films were dried, each composite film was pressed against a pure polymer film using a uniaxial press using 2 tons of force at 80 °C in a stainless steel mold. The resulting bilayer films showed good adhesion to one another.

#### **4.4.2 Testing pressed films**

The 60 wt% CNC film showed a good degree of actuation in a short time (as shown in figure 4.1); however, the actuation was only semi-reversible and did not reactuate. None of the other films showed as drastic of a result, though almost all films did have some actuation. I believe that the high level of CNCs increased the amount of water that could be held in the composite. As the amount of water that the composite held increased, so did the actuation. The 90 wt% film did not have enough polymer to hold the CNCs in and I noticed loose CNCs in the water. Once dried, the CNCs did start to move back to their original shape, but stayed partially bent.



Figure 4.1: 60 wt % CNC film before water was added (left), 15 minutes after water was added (center), and one hour after water was added.

The first problem was that the film did not bend back all the way, especially at high concentrations of CNCs. I believe that the composites started to bend back as the water left, but the composite became more stiff as the water left and the stiffness increased again. Unfortunately, the film becomes too stiff to totally return to its original shape. I determined that I need to make films with less than 20 wt% CNCs because films with more than that did not fully reverse actuation. In order to increase the amount of movement with lower water intake, more interface area could be used to increase the bending angle.

## 4.5 3D printing

### 4.5.1 Preparing printing films

Several designs were considered to create a structure with a larger interface between the pure Texin TPU and the CNC composite. Eventually, a structure where a block of composite surrounded on three sides by pure TPU was decided upon. This design was chosen for its relative ease of manufacturing combined with its high interface area. A model of the design is shown below in figure 4.2.

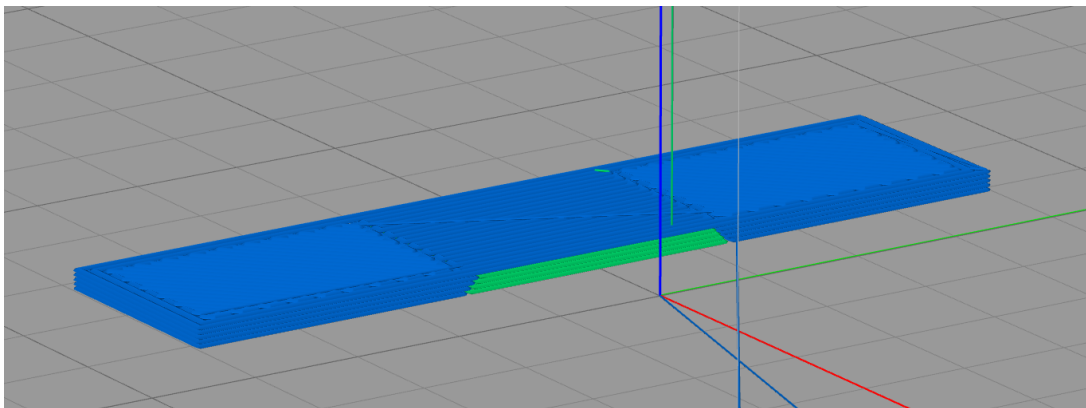


Figure 4.2: A computer model showing the structure of the bi-layer film. The green area represents the CNC composite while the blue area shows pure polyurethane.

In order to make the relatively more complex design, I determined that extrusion-based additive manufacturing would be the best method. I chose this method because it

is relatively easy to make many different sample geometries, Convestro recommends extrusion to process Texin, and Dr. Bortner's research group has done research with CNC/Texin composites using such printers. I used the same method as discussed in section 4.4.1 to make a larger batch of 20 wt% CNC composite. The resulting film was chopped into pellets and extruded at 190 °C to make a filament for printing. A creator pro flash forge dual extrusion 3D printer was used to print the structure. The goal was to print several thicknesses of the composite part to determine the effect that layer thickness had on degree of actuation. Because the part was 10 layers thick, I was going to have 11 samples from 0 to all 10 layers as composite. The samples were printed at a temperature of 230 °C for the best result.

#### 4.5.2 Testing printed films

The films were obviously degraded but were tested for actuation despite the appearance. Figure 4.3 shows the degree of actuation after several days in DI water.

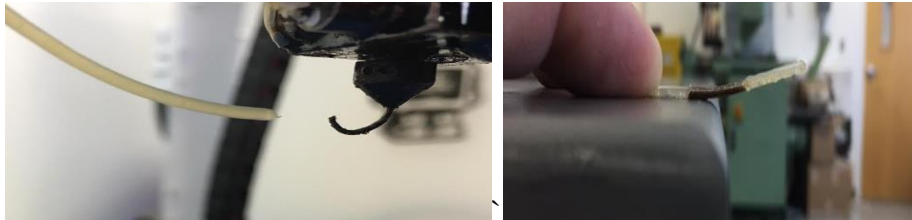


Figure 4.3: Composite filament before and after printing (left), and printed around TPU in a bi-layer film in its actuating state (right).

The films actuated to about 8 degrees using 7 layers of composite and 3 layers of pure TPU. The Texin printed well with few problems. The high temperatures degraded the CNCs significantly leading to the black color. Lower printing temperatures were tried but the composite became too viscous to print. Printing was done in different atmospheres, including nitrogen and argon environments, to prevent some degradation, but neither atmosphere prevented the print from turning black.

The obvious problem with this was the fact that the cellulose degraded significantly. Despite attempts to use different environments, the films could not be printed without degrading the cellulose. The films did not bend very much due to the lack of hydrogen bonds. We determined that using a TPU with a lower processing temperature as well as making phosphate CNCs (p-CNCs), which have a higher degradation temperature, would allow us to print

### **4.5.3 Changing the materials**

p-CNCs were isolated based on the procedure outlined by Sandra et al.<sup>27</sup> Whatman filter paper was blended in a kitchen blender with 50 mL of water per gram of paper. While in an ice bath, phosphoric acid was added dropwise to the cellulose pulp until the concentration reached 10.7 M. Once the acid had been added, the mixture was heated to 100 °C for 90 minutes. The isolated p-CNCs were removed by centrifuging and decanting the mixture 3 times and the remaining acid was removed by dialysis for a week exchanging the water daily. The isolated p-CNCs were a tan color and dispersed well in water. The CNCs were characterized by thermogravimetric analysis as shown in figure 4.4. There was a single degradation curve with an onset of thermal degradation at 258 °C, which corresponds well with other p-CNC data, indicating that the p-CNCs were successfully isolated.<sup>27</sup>

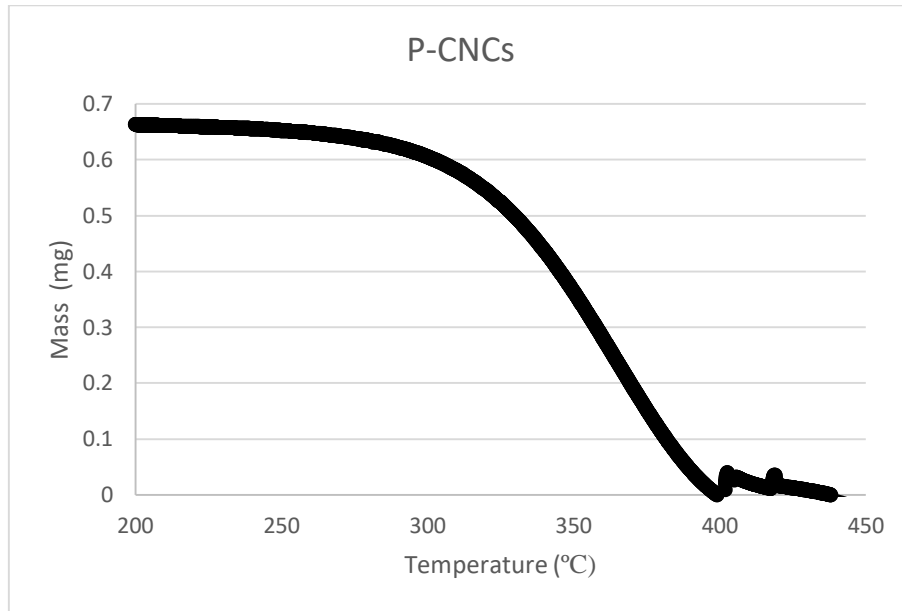


Figure 4.4: TGA of isolated CNCs

Capillary rheometry was done to determine if the Elastollan Soft 35 can indeed be processed at a lower temperature than the Texin. Figure 4.5 shows that at the same temperatures and shear rates, the Soft 35 has significantly lower viscosity than the Texin.

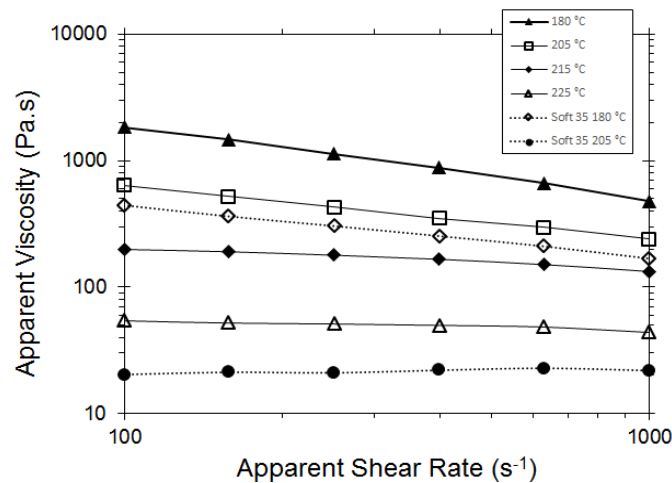


Figure 4.5: Capillary rheometry of Texin and Soft 35 at various temperatures.

Composites were made out of the isolated CNCs and Elastollan Soft 35. This polyurethane was chosen because of its lower processing temperature. The CNCs were transferred to water by first centrifuging and decanting most of the water, replacing it

with DMF. The remainder of the water was removed by boiling the mixture at 110 °C for an hour. Composites were made as described in section 4.4.1 and extruded into filament as discussed in section 4.5.1. The filament was 10 wt% CNC. The Soft 35 films were printed under the same conditions as the Texin films.

Due to the low modulus of the Soft 35, it bent before it could be successfully extruded, so no films were printed. In order to continue working with the new TPU, I decided to use a stainless steel mold, uniaxially hot-press the films as two separate parts and, use DMF to adhere the two parts together.

## **4.6 Compression molding**

### **4.6.1 Preparing molded samples**

In order to pursue this process, I again solution cast films of Soft 35 using the commercially available CNCs. Using the same procedure from section 4.4.1, a film was cast with 10 wt% CNCs. Compression molds were created by the chemical engineering machine shop and are shown in figure 4.6. The two components were pressed at 9 tons and 80 °C.

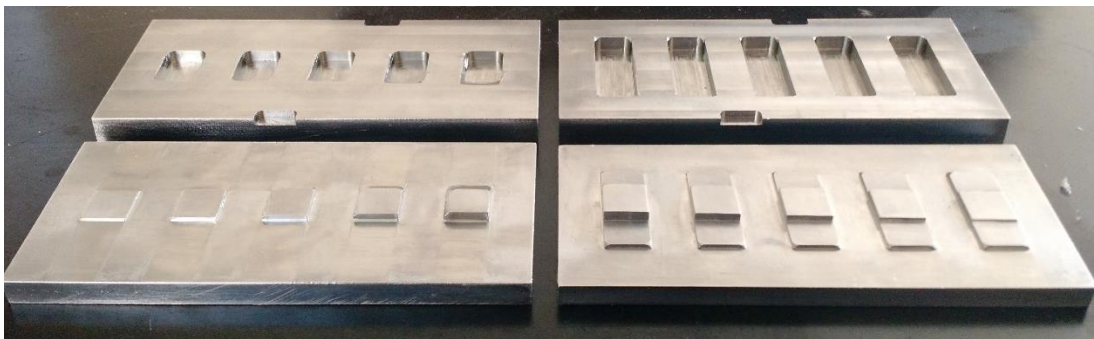


Figure 4.6: Custom steel compression mold.



The resulting films showed significant darkening from thermal degradation. To combat this, DMF was added to the composites as a plasticizer. This allowed the Soft 35 to flow at lower temperatures so the CNCs were not degraded.

#### **4.6.2 Testing compression molded films**

The parts appeared properly shaped, so they were tested in water. Although there was some actuation, due to the low CNC content of the composite necessary to process them, the actuation was nearly unmeasurably small at around 1 degree of bending.

Because the polymer has to flow freely in the mold, the processing temperature was too high for the CNCs despite the added plasticizer. There was not enough time to do studies to see how much additive would be needed to increase the volume of CNCs and get a better response. It is also unclear at this point if the plasticizer would have any effect on the swelling behavior.

#### **4.7 Modeling**

Using the equations above, I decided to see how much actuation we should expect from CNC/TPU composites. Swelling tests were done using films cast from Soft 35 and 0, 5, 10, and 15 wt% of the commercially available CNCs. The films were cast as described in section 4.4.1. In order to use equation 4.2, which models swelling-based composites, the degree of swelling and the Young's modulus need to be found for various concentration of CNCs.

Swelling behaviors varied by CNC concentration and time. Samples were dried for 1 hour in a vacuum oven at 80 °C and 20 in Hg. After that, they were weighed and placed into water. Every 6 minutes for half an hour, the samples were removed from the water, dried on paper towels, and weighed. The Young's modulus was found through

dynamic mechanical analysis (DMA) in tension. Dog bone shapes were cut from the films via a manual press and tested on a TA Q800 by increasing the force by 0.5 N/min.

As expected, the weight gain from water and stiffness increased as the volume of CNCs increased. There was a significant difference between the 0, 5, and 10 wt% CNC samples, but not a significant increase in the 15 wt% CNC sample. I believe that this is because the CNCs have already created a network by the 10 wt% mark, so water can more easily reach most of the cellulose without having to pass through the TPU. I still believe that increasing the amount of cellulose will continue to increase the weight gain from water. Figure 4.7 shows the percent weight gain over time, as well as the mechanical testing discussed previously.

With all of the properties of the films characterized, equation 4.2 was used to create a series of predictions of the maximum height that a 1 cm long film would reach if exposed to water for 30 minutes. This is also shown in figure 4.7 on the next page. Based on these models, the 10% CNC films actually should have the highest actuation at most thicknesses. I believe this is due to the swelling data being comparable for the 10 and 15 wt%, with much higher stiffness for the 15%. I believe that if more composites were tested, composites with more CNCs would actuate more than the 10%, based on my tests done earlier with 60 wt %.

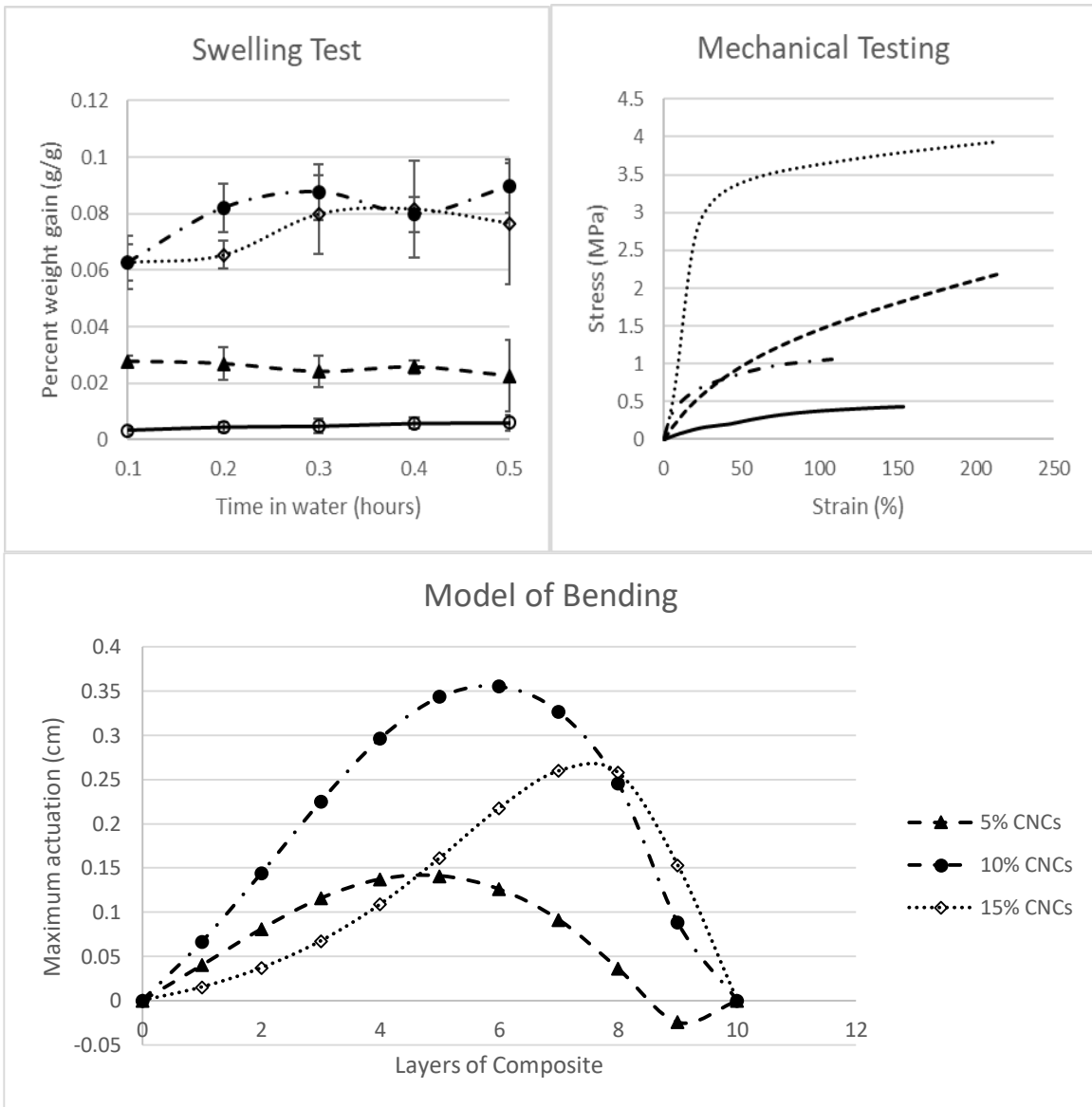


Figure 4.7: a) Percent mass gained after various times in water, b) Mechanical testing of different wt% CNC composites, c) Maximum actuation of different thicknesses of different concentrations of CNC composites.

#### 4.8 Future recommendations

I still believe that it is possible to make a water-actuating film based on the swelling behaviors of CNCs in TPU. I believe that using additives will help to lower the printing temperature of higher percent CNC composites that will be able to show good actuation. There are several good plasticizers to choose from for TPUs. I used DMF because it was readily available to me in a short amount of time, and it works well, but

because at higher temperatures it can evaporate and cause health problems, I do not recommend using it in this project without good ventilation.<sup>28</sup> A much better option appears to be Benzoflex, a benzoate ester that is commonly recommended and lacks many of the same health hazards as DMF. There has been research into even less dangerous additives for polyurethanes, such as diurethanes, that can reduce the processing temperature and can provide other improvements such as increased strength.<sup>29</sup> I believe that after studying the effects of such plasticizers, it could lower the melt viscosity of the CNC/TPU composites enough that even higher weight percents can be printed without thermal degradation.

By reducing the printing temperature, higher wt% CNC composites can also be printed without degrading. I would not recommend going all the way up to 60% CNC due to the lack of reversibility. The first goal should be to use plasticizers to print a 20% CNC composite. Once that is accomplished, then studies can be done to determine the effects of layer thickness and amount of cellulose on bending action. Other studies could be done to determine if the plasticizer changes the stiffness or swelling behaviors of the polyurethanes.

When films finally do get made, I expect to see higher wt % CNC composites flex more, especially at higher thicknesses, but be less reverseable. Being able to change the deflection by both concentration and thickness will help to optimize the material for potential stiffness and actuation requirements.

#### **4.9 References**

1. Bakarich, S. E.; Bakarich, S. E.; Gorkin, R.; Panhuis, M. i. h.; Spinks, G. M., 4D Printing with Mechanically Robust, Thermally Actuating Hydrogels. *Macromolecular rapid communications*. 36 (12), 1211-1217.

2. Liu, Y.; Shaw, B.; Dickey, M. D.; Genzer, J., Sequential self-folding of polymer sheets. *Science Advances* **2017**, *3* (3).
3. Käpylä, E.; Delgado, S. M.; Kasko, A. M., Shape-Changing Photodegradable Hydrogels for Dynamic 3D Cell Culture. *ACS Applied Materials & Interfaces* **2016**, *8* (28), 17885-17893.
4. Felton, S. M.; Tolley, M. T.; Shin, B.; Onal, C. D.; Demaine, E. D.; Rus, D.; Wood, R. J., Self-folding with shape memory composites. *Soft Matter* **2013**, *9* (32), 7688-7694.
5. Kokkinis, D.; Schaffner, M.; Studart, A. R., Multimaterial magnetically assisted 3D printing of composite materials. *Nature Communications* **2015**, *6*, 8643.
6. Tibbits, S., 4D Printing: Multi-Material Shape Change. *Architectural design* **84** (1), 116-121.
7. Headrick, D., 4D printing transforms product design. *Research Technology Management* **2015**, *58* (2), 7.
8. Gargava, A.; Arya, C.; Raghavan, S. R., Smart Hydrogel-Based Valves Inspired by the Stomata in Plants. *ACS Applied Materials & Interfaces* **2016**, *8* (28), 18430-18438.
9. Zirbel, S. A.; Zirbel, S. A.; Lang, R. J.; Thomson, M. W.; Sigel, D. A., Accommodating thickness in origami-based deployable arrays. *Journal of mechanical design (1990)* **135** (11), 111005.
10. Onal, C. D.; Onal, C. D.; Tolley, M. T.; Wood, R. J.; Rus, D., Origami-Inspired Printed Robots. *IEEE/ASME transactions on mechatronics* **2014**, *20* (5), 1-8.
11. Morgan, M. R.; Lang, R. J.; Magleby, S. P.; Howell, L. L., Towards developing product applications of thick origami using the offset panel technique. *Mech. Sci.* **2016**, *7* (1), 69-77.
12. Nelson, T. G.; Lang, R. J.; Magleby, S. P.; Howell, L. L., Curved-folding-inspired deployable compliant rolling-contact element (D-CORE). *Mechanism and Machine Theory* **2016**, *96*, Part 2, 225-238.
13. Yan Nai, T.; Herder, J. L.; Tuijthof, G.; Ile, J. M., Steerable Mechanical Joint for High Load Transmission in Minimally Invasive Instruments. *Journal of medical devices* **2011**, *5* (3), 34503.
14. Nuwer, R., Microscopic origami machine toggles between folded and unfolded states. *MRS Bulletin* **2015**, *40* (6), 462.
15. Kuo, J.-N.; Lee, G.-B.; Pan, W.-F.; Lee, H.-H., Shape and Thermal Effects of Metal Films on Stress-Induced Bending of Micromachined Bilayer Cantilever. *Japanese journal of applied physics* **44** (5a), 3180-3186.
16. Mehnen, L.; Mehnen, L.; Pf; uuml; tzner, H.; Kaniusas, E., Magnetostrictive amorphous bimetal sensors. *Journal of magnetism and magnetic materials* **2000**, *215*, 779-781.
17. Arnaud, A.; Arnaud, A.; Boughaleb, J.; Monfray, S.; Boeuf, F., Description of the performances of a thermo-mechanical energy harvester using bimetallic beams. *Optical materials* **56**, 75-79.
18. Kim, D.-G.; Kim, D.; Gil; Kang, H.; Pan, J.; Kyung; Kim, Y.; Chon, Sensitivity enhancement of a fiber grating temperature sensor combined with a bimetallic strip. *Microwave and optical technology letters* **56** (8), 1926-1929.

19. Abu-Lail, N. I.; Kaholek, M.; LaMattina, B.; Clark, R. L.; Zauscher, S., Micro-cantilevers with end-grafted stimulus-responsive polymer brushes for actuation and sensing. *Sensors and Actuators B: Chemical* **2006**, *114* (1), 371-378.
20. Clyne, T. W.; Clyne, T. W., Residual Stresses in Surface Coatings and Their Effects on Interfacial Debonding. *Key engineering materials* **1996**, *116-117*, 307-330.
21. Guan, J.; He, H.; Hansford, D. J.; Lee, L. J., Self-Folding of Three-Dimensional Hydrogel Microstructures. *The Journal of Physical Chemistry B* **2005**, *109* (49), 23134-23137.
22. He, S.; Chen, P.; Qiu, L.; Wang, B.; Sun, X.; Xu, Y.; Peng, H., A Mechanically Actuating Carbon-Nanotube Fiber in Response to Water and Moisture. *Angewandte Chemie (International ed. in English)* **2015**, *54* (49), 14880-14884.
23. Mendez, J.; Annamalai, P. K.; Eichhorn, S. J.; Rusli, R.; Rowan, S. J.; Foster, E. J.; Weder, C., Bioinspired mechanically adaptive polymer nanocomposites with water-activated shape-memory effect. *Macromolecules* **2011**, *44* (17), 6827-6835.
24. Annamalai, P. K.; Dagnon, K. L.; Monemian, S.; Foster, E. J.; Rowan, S. J.; Weder, C., Water-Responsive Mechanically Adaptive Nanocomposites Based on Styrene-Butadiene Rubber and Cellulose Nanocrystals—Processing Matters. *ACS Applied Materials & Interfaces* **2014**, *6* (2), 967-976.
25. Dufresne, A., *Nanocellulose: from nature to high performance tailored materials*. De Gruyter: Berlin;Boston, 2012; Vol. 1. Aufl.
26. Díez-Peña, E.; Quijada-Garrido, I.; Barrales-Rienda, J. M., Hydrogen-Bonding Effects on the Dynamic Swelling of P(N-iPAAm-co-MAA) Copolymers. A Case of Autocatalytic Swelling Kinetics. *Macromolecules* **2002**, *35* (23), 8882-8888.
27. Camarero Espinosa, S.; Kuhnt, T.; Foster, E. J.; Weder, C., Isolation of Thermally Stable Cellulose Nanocrystals by Phosphoric Acid Hydrolysis. *Biomacromolecules* **2013**, *14*, 1223-1230.
28. Kim, T. H.; Kim, S. G., Clinical outcomes of occupational exposure to n,n-dimethylformamide: perspectives from experimental toxicology. *Safety and health at work* **2011**, *2* (2), 97-104.
29. Tereshatov, V. V.; Senichev, V. Y., New diurethane plasticizers for polyurethane thermoplastics and perspective functional composites. *Journal of applied polymer science* *132* (7), n-a-n/a.

## **Chapter 5: Conclusions**

### **5.3 Conclusions**

This thesis has found a number of conclusions. The first is that cellulose nanocrystals (CNCs) can be isolated from pistachio shells. We have further determined that the CNCs thusly isolated had a high aspect ratio, low crystallinity, and low surface charge density. We reported a procedure for high-yield isolation of the CNCs from pistachio shells utilizing sulfuric acid hydrolysis. We further discovered that such CNCs can be used to reinforce composites.

We have also concluded that CNC composites can, if structured properly, be used to create a smart composite. Such a material will bend when water is added due to the swelling behaviors of the different components of the system. Although there is more work to be done to find the correct method for processing the composite using plasticizers, I believe that it should be very possible.

### **5.2 Outlook**

Despite not having finalized the method of creating an actuating film, this thesis was successful in both of its goals. I did manage to find a new source material for CNCs, and we did determine a novel use for CNCs in creating a water-actuating hinge. I hope that this work will improve the market for CNCs by providing pistachio shells as a new viable, high yield feedstock material. I also hope that creating new and exciting uses for CNC-based composites will help grow the demand for CNCs. More work in both of these categories will further help to grow the market for CNCs and help their commercialization.